AD_____

Award Number: DAMD17-99-1-9069

TITLE: Mouse Mammary Cancer Models - Mechanisms and Markers

PRINCIPAL INVESTIGATOR: Lawrence Donehower, Ph.D.

CONTRACTING ORGANIZATION: Baylor College of Medicine
Houston, Texas 77030

REPORT DATE: August 2000

TYPE OF REPORT: Annual Summary

PREPARED FOR: U.S. Army Medical Research and Materiel Command
Fort Detrick, Maryland 21702-5012

DISTRIBUTION STATEMENT: Approved for Public Release;
Distribution Unlimited

The views, opinions and/or findings contained in this report are those of the author(s) and should not be construed as an official Department of the Army position, policy or decision unless so designated by other documentation.

REPORT DOCUMENTATION PAGE

Form Approved
OMB No. 074-0188

1. AGENCY USE ONLY (Leave blank)	2. REPORT DATE	3. REPORT TYPE AND DATES COVERED
	August 2000	Annual Summary (1 Aug 99 - 31 Jul 00)

4. TITLE AND SUBTITLE
Mouse Mammary Cancer Models - Mechanisms and Markers

5. FUNDING NUMBERS
DAMD17-99-1-9069

6. AUTHOR(S)
Lawrence Donehower, Ph.D.

7. PERFORMING ORGANIZATION NAME(S) AND ADDRESS(ES)
Baylor College of Medicine
Houston, Texas 77030

E-MAIL:
larryd@bcm.tmc.edu

8. PERFORMING ORGANIZATION REPORT NUMBER

9. SPONSORING / MONITORING AGENCY NAME(S) AND ADDRESS(ES)
U.S. Army Medical Research and Materiel Command
Fort Detrick, Maryland 21702-5012

10. SPONSORING / MONITORING AGENCY REPORT NUMBER

11. SUPPLEMENTARY NOTES

12a. DISTRIBUTION / AVAILABILITY STATEMENT
Approved for public release; distribution unlimited

12b. DISTRIBUTION CODE

13. ABSTRACT ***(Maximum 200 Words)***

We have focused on two mouse models for mammary cancer, the p53-deficient *Wnt-1* transgenic model and the *Chk1*-deficient *Wnt-1* transgenic model. Both bitransgenic models are dependent on the *Wnt-1* transgene to initiate mammary adenocarcinomas within 3-12 months after birth. Our goal was to determine what effect deficiency of the p53 tumor suppressor or the cell G2 checkpoint gene *Chk1* would have on*Wnt-1* initiated mammary tumorigenesis. Characterization of the biology of the p53-deficient *Wnt-1* transgenic model had shown that p53-/- mice develop tumors that arise sooner, grow faster, have more anaplastic histopathology, and have more chromosomal instability than p53+/+ mice. To identify genes which might be involved in the different tumor phenotypes, we compared their global RNA expression patterns by various approaches. We identified six genes consistently upregulated in p53+/+ mammary tumors and one consistently upregulated in p53-/- tumors. All of these genes are relevant either to cell cycle control or differentiation state and may in part be responsible for the less aggressive p53+/+ tumor phenotypes. Comparison of tumor incidence in the *Chk1*+/- and *Chk1*+/+ *Wnt-1* transgenic mice revealed a significantly earlier appearance of *Chk1*+/- tumors, consistent with the hypothesis that Chk1 is a real tumor suppressor.

14. SUBJECT TERMS
Breast Cancer, mouse mammary cancer models, p53, Chk1, Wnt-1

15. NUMBER OF PAGES
54

16. PRICE CODE

17. SECURITY CLASSIFICATION OF REPORT	18. SECURITY CLASSIFICATION OF THIS PAGE	19. SECURITY CLASSIFICATION OF ABSTRACT	20. LIMITATION OF ABSTRACT
Unclassified	Unclassified	Unclassified	Unlimited

Table of Contents

INTRODUCTION:

During the last year of this Academic Award Period, we have focused on the characterization of two mouse models for mammary cancer, the p53-deficient *Wnt-1* transgenic model and the *Chk1*-deficient *Wnt-1* transgenic model. Both of these bitransgenic models are dependent on the *Wnt-1* transgene to initiate mammary adenocarcinomas in the females within 3-12 months after birth. Our goal was to determine what effect either deficiency of the p53 tumor suppressor gene or of the cell G2 cell cycle checkpoint control gene *Chk1* would have on the progression of the *Wnt-1* initiated mammary tumors. We had already extensively characterized the biology of the p53-deficient *Wnt-1* transgenic model and shown that mice null for p53 develop tumors that arise sooner, grow faster, have more anaplastic histopathology, and have more chromosomal instability than mice with intact p53. To identify genes which might be involved in the different tumor phenotypes of the p53-/- and p53+/+ mammary tumors, we compared their global RNA expression patterns by differential display, cDNA array, and candidate gene approaches. In our initial experiments, we identified six genes which are consistently upregulated in p53+/+ mammary tumors and one consistently upregulated in p53-/- tumors. All of these genes are relevant either to cell cycle control or differentiation state and may in part be responsible for the less aggressive tumor phenotype of the p53+/+ tumors. Comparison of the tumor incidences of the *Chk1*+/- and *Chk1*+/+ *Wnt-1* transgenic mice revealed a significantly earlier appearance of *Chk1*+/- tumors. This result was consistent with the hypothesis that Chk1 is a bona fide tumor suppressor.

BODY:

RESEARCH ACCOMPLISHMENTS:

I. Differential Gene Expression in Mammary Tumors from p53+/+ and p53-/- *Wnt-1* Transgenic Mice

For several years we have been comparing the biology and genetics of the mammary tumors arising in our bitransgenic model, the p53-defcient *Wnt-1* transgenic mouse. We had developed this model because our original model, the p53-deficient mouse, rarely developed mammary tumors. In order to investigate the role of p53 loss in mammary tumorigenesis, we crossed the p53 mutation into the *Wnt-1* transgenic mouse obtained from Harold Varmus. The *Wnt-1* transgenic females reliably develop mammary carcinomas within 3-12 months after birth. We found that p53-/- *Wnt-1* transgenic females develop mammary tumors that arise sooner, grow faster, have more anaplastic histopathology, and have more chromosomal instability than their p53+/+ counterparts. The table below summarizes some of the biological and genetic differences between p53+/+ and p53-/- *Wnt-1* tumors.

Table I. Biological and genetic properties of *Wnt-1* TG p53+/+ and *Wnt-1* TG p53-/- mammary adenocarcinomas

Property	p53+/+	p53-/-
Tumor type	mammary adenocarcinoma	mammary adenocarcinoma
50% tumor incidence	22.5 weeks	11.5 weeks
100% tumor incidence	40 weeks	15 weeks
Mean tumor growth rate	800 cu. mm/wk	3400 cu. mm/wk
Mean percentage of mitotic tumor cells	.0027	.0070
Mean percentage of apoptotic tumor cells	0.32	0.48
Percentage of tumors with abnormal chromosomes	33	100
Mean number of abnormal chromosomes per tumor	0.3	1.7
Histopathological appearance	uniform nuclei differentiated more stroma	anaplastic undifferentiated less stroma

To understand some of the molecular mechanisms which underlie the differences in biological phenotypes between the p53+/+ and p53-/- *Wnt-1* transgenic mammary tumors, we compared their global RNA expression patterns by differential display PCR, cDNA array, and candidate gene approaches utilizing Northern blot and RNAse protection analyses. To be certain that the differentially expressed genes that we initially identified were a result of the presence or absence of p53 and not a result of intertumor variation, we examined eight distinct p53-/- and eight p53+/+ tumor RNA samples. All differential expression results obtained by differential display PCR and cDNA array analyses were confirmed by Northern blot hybridization and in many cases by Western blot analyses to show that protein expression levels were altered. As shown below in Table II, seven genes were identified that showed significant levels of differential expression between p53+/+ and p53-/- tumor types.

Table II. Differentially expressed genes in *Wnt-1* TG p53+/+ and *Wnt-1* TG p53-/- mammary adenocarcinomas

Gene	ID method	p53+/+ levels	p53 target?	Function/Marker
Alpha smooth muscle actin	Diff. Display	Increased	Yes	myoepithelial cell marker
Kappa casein	Diff. Display	Increased	No	luminal cell epithelial marker
c-kit	cDNA Array	Increased	No	receptor tyrosine kinase
Cytokeratin 19	cDNA Array	Increased	Yes	epithelial cell intermediate filament marker
$P21^{WAF1/CIP1}$	Northern	Increased	Yes	cdk inhibitor growth marker
Cyclin B1	RNAse Prot.	Decreased	Yes (neg.)	mitotic cyclin growth marker
Cyclin G1	RNAse Prot.	Increased	Yes	function unclear

In examining the differentially expressed genes that have so far been identified in this tumor model, certain trends have emerged. First, all of the differentially expressed genes fall into one of two categories, either growth-related cell cycle control genes or differentiation-related genes. The differentiation-related genes (alpha smooth muscle actin, cytokeratin 19, and kappa casein) were all expressed at higher levels in the p53+/+ tumors, consistent with their more differentiated histopathological phenotypes. The cell cycle control genes or growth related genes (p21, cyclin B1, cyclin G1, c-kit) were also expressed in a manner consistent with the tumor cell growth rates observed in the parental tumors. For example the cyclin-dependent kinase inhibitor p21 was expressed at higher levels in p53+/+ tumors, suggesting that the increased expression of this protein may in part be responsible for the reduced cell cycle progression seen in these tumors compared to their p53-/- counterparts. The increased c-kit expression in p53+/+ tumors actually mirrored the observation that human breast cancers showed a reduction in c-kit expression as the cancer progressed from benign lesions to more malignant forms. Thus, our p53+/+ tumors are likely to represent a more benign stage of mammary tumor progression, while the p53-/- tumors may be models for the more invasive stages of mammary carcinomas.

A second interesting observation was the fact that five of the seven differentially expressed genes were known target genes of p53. This indicates that the p53+/+ tumors did have intact p53 signaling and it suggests that p53 signaling may be regulating tumor growth and differentiation-associated targets in a manner that directly contributes to the observed biological phenotypes.

We are in the process of performing further screens with larger cDNA arrays. These should reveal additional differentially expressed genes. A remaining challenge will be to determine which of these differentially expressed genes have a direct effect on the biological properties of the mammary adenocarcinomas.

II. Differential Tumor Incidence in Chk1+/- and Chk1+/+ *Wnt-1* Transgenic Mice

Our success in using the *Wnt-1* transgenic model as an assay system for the role of tumor suppressor genes (and putative tumor suppressor genes) in a mammary cancer context led us to test the possibility that a newly identified cell cycle checkpoint gene, *Chk1*, was in fact a tumor suppressor. This work was carried out in collaboration with Steve Elledge, the discoverer of the *Chk1* gene. Chk1 is an evolutionarily conserved kinase and has been implicated in G2 cell cycle checkpoint control in yeast and mammalian cells. The p53 protein has also been shown to be a phosphorylation target of Chk1 following DNA damage. The Elledge lab has generated *Chk1*+/- mice through ES cell targeting methods. *Chk1* nullizygosity is an early embryonic lethal condition. We crossed the *Chk1*+/- mice obtained from the Elledge lab to our *Wnt-1* transgenic mice and compared the mammary tumor incidences between *Chk1*+/- females and *Chk1*+/+ females. We hypothesized that if *Chk1*+/- females developed tumors earlier than *Chk1*+/+ females then this would provide suggestive evidence that Chk1 is a bona fide tumor suppressor gene. After monitoring 22 *Chk1*+/+ and 22 *Chk1*+/- females for almost a year we obtained the tumor incidence curve shown on the next page in Figure 1. Note that the *Chk1*+/- mice do develop tumors earlier than the *Chk1*+/+ mice. Statistical comparison of the tumor

incidences did reveal a statistically significant difference in these curves. Thus, it is likely that Chk1 does have tumor suppressor function.

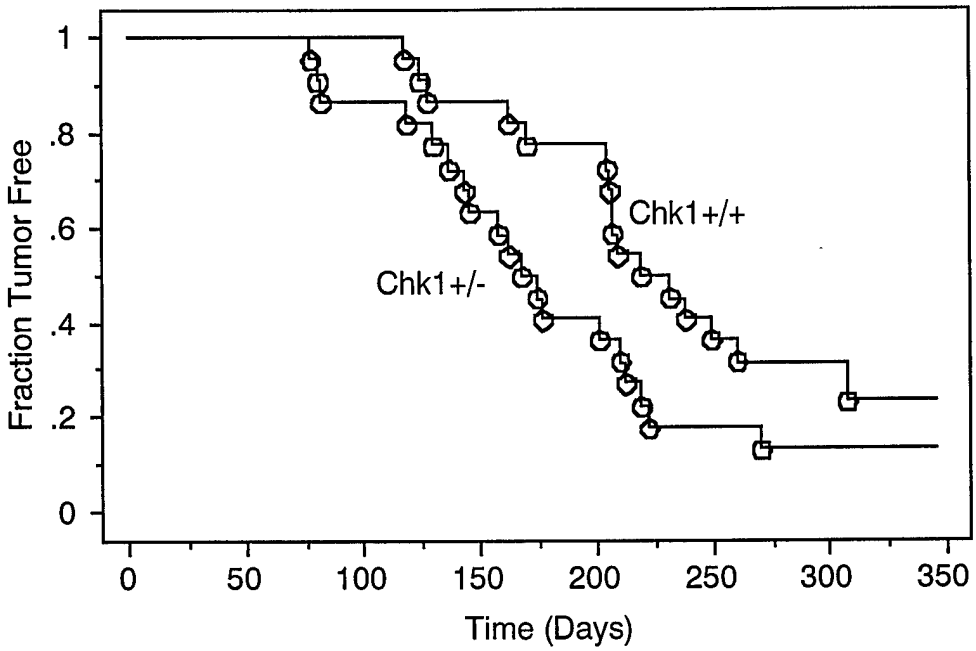

Figure 1. Mammary tumor incidence in *Chk1*+/- and *Chk1*+/+ *Wnt-1* transgenic females.

APPENDIX:

List of Key Research Accomplishments

(1) Identification of seven differentially expressed genes in mammary tumors derived from p53+/+ and p53-/- mice.

(2) Demonstration that the newly identified cell cycle checkpoint gene is likely to be a tumor suppressor in a mouse mammary tumor model context

List of Reportable Outcomes

(1) Two manuscripts (appended)

(a) Lui, Q., Guntuku, S., Cui, X., Matsuoka, S., Cortez, D., Tamai, K., Luo, G., Carattini-Rivera, S., DeMayo, F., Bradley, A., Donehower, L.A., and Elledge, S.J. (2000). CHK1 is an essential gene that is regulated by Atr and required for the G2/M DNA damage checkpoint. Genes & Dev. 14, 1448-145.

(b) Cui, X. and Donehower, L.A. (2000). Differential gene expression in murine mammary tumors in the presence and absence of p53 (submitted).

Chk1 is an essential kinase that is regulated by Atr and required for the G_2/M DNA damage checkpoint

Qinghua Liu,[1-3] Saritha Guntuku,[1,2] Xian-Shu Cui,[4] Shuhei Matsuoka,[1,2] David Cortez,[1,2] Katsuyuki Tamai,[7] Guangbin Luo,[1,5] Sandra Carattini-Rivera,[1,5] Francisco DeMayo,[6] Allan Bradley,[1,5] Larry A. Donehower,[4,6] and Stephen J. Elledge,[1,2,5,8]

[1]Howard Hughes Medical Institute, [2]Verna and Marrs McLean Department of Biochemistry, [3]Program in Cell and Molecular Biology, [4]Department of Molecular Virology and Microbiology, [5]Department of Molecular and Human Genetics, and [6]Department of Molecular and Cellular Biology, Baylor College of Medicine, Houston, Texas 77030 USA; [7]Medical and Biological Laboratories Co., Ltd., Ina, Nagano 396-0002, Japan

Chk1, an evolutionarily conserved protein kinase, has been implicated in cell cycle checkpoint control in lower eukaryotes. By gene disruption, we show that *CHK1* deficiency results in a severe proliferation defect and death in embryonic stem (ES) cells, and peri-implantation embryonic lethality in mice. Through analysis of a conditional *CHK1*-deficient cell line, we demonstrate that ES cells lacking Chk1 have a defective G_2/M DNA damage checkpoint in response to γ-irradiation (IR). *CHK1* heterozygosity modestly enhances the tumorigenesis phenotype of *WNT-1* transgenic mice. We show that in human cells, Chk1 is phosphorylated on serine 345 (S345) in response to UV, IR, and hydroxyurea (HU). Overexpression of wild-type Atr enhances, whereas overexpression of the kinase-defective mutant Atr inhibits S345 phosphorylation of Chk1 induced by UV treatment. Taken together, these data indicate that Chk1 plays an essential role in the mammalian DNA damage checkpoint, embryonic development, and tumor suppression, and that Atr regulates Chk1.

[*Key Words*: Atr; Atm; Chk1; embryonic lethality; DNA damage; checkpoint]

Received March 20, 2000; revised version accepted May 1, 2000.

The ability of organisms to sense and respond to DNA damage is critical for their long-term survival. Consequently, cells have evolved an elaborate DNA damage response pathway that senses aberrant DNA structures and transmits a damage signal to effectors that act to enhance survival of the organism (Elledge 1996). Activation of the DNA damage response pathway results in transcriptional induction of genes involved in DNA repair, activation of DNA repair pathways, and arrest of cell cycle progression. In metazoans, cells experiencing DNA damage may also undergo apoptotic cell death, thereby preventing these cells from possibly contributing to tumorigenesis or other diseases. Because many genes involved in the regulation of DNA damage responses were originally identified based on their ability to control cell cycle progression, the DNA damage response pathway is also often referred to as the DNA damage checkpoint pathway.

The mammalian DNA damage response pathway consists of several families of conserved protein kinases. Two members of the phosphoinositol kinase (PIK) family, Atm and Atr, are at the top of this signal transduction cascade. Although related, Atm and Atr form two distinct subfamilies in evolution. Atm is more closely related to Tel1 in *Saccharomyces cerevisiae* and *Schizosaccharomyces pombe*, whereas Atr (Cimprich et al. 1996; Keegan et al. 1996) is more closely related to Mec1 in *S. cerevisiae*, Rad3 in *S. pombe*, and Mei-41 in *Drosophila melanogaster* (for review, see Elledge 1996). The *ATM* gene is mutated in the familial neural degeneration and cancer-predisposition syndrome ataxia telangiectasia (Savitsky et al. 1995). *ATM* deficient mice are viable, but show growth retardation, infertility, and cancer predisposition (Barlow et al. 1996; Xu et al. 1996). *ATM* mutant cells are defective for DNA damage checkpoints and are very sensitive to agents that cause double-stranded DNA breaks, such as γ-irradiation (IR). Like *ATM* mutant cells, yeast *tel1* mutants have short telomeres, but they have intact cell cycle checkpoints and display only limited sensitivity to DNA-damaging agents. Less is known about Atr due to a lack of *ATR* mutant cells. However, overexpression of a kinase-defective Atr mutant abrogates cell cycle arrest after DNA damage, revealing a role in DNA damage checkpoints (Cliby et al. 1998; Wright et al. 1998). *ATR* disruption in mice results in peri-implantation embryonic lethality and fragmented chromosomes (Brown and Baltimore 2000). In *D. melanogaster*, *mei-41* mutant embryos cannot properly lengthen the cell cycle at the midblastula

[8]Corresponding author.
E-MAIL selledge@bcm.tmc.edu; FAX (713) 798-8717.

transition and this leads to embryonic lethality (Sibon et al. 1999).

Downstream of Atm and Atr are two families of protein kinases, Chk1 and Chk2. The Chk2 family consists of Rad53 in *S. cerevisiae* and Cds1 in *S. pombe* (for review, see Elledge 1996), and Chk2/Cds1 in mouse and human (Matsuoka et al. 1998; Blasina et al. 1999; Brown et al. 1999; Chaturvedi et al. 1999). The Chk2 family kinases can be activated by DNA damage or replication blocks and this activation requires upstream PIK members in their respective species (Sanchez et al. 1996; Sun et al. 1996; Boddy et al. 1998; Lindsay et al. 1998). Chk2 is involved in DNA damage checkpoints because Chk2-deficient embryonic stem (ES) cells fail to maintain G_2 arrest after DNA damage (Hirao et al. 2000). *CHK2*$^{-/-}$ thymocytes are resistant to IR-induced apoptosis and fail to stabilize and activate p53 in response to IR (Chehab et al. 2000; Hirao et al. 2000).

The Chk1 kinase family consists of Chk1 in *S. pombe* (Walworth et al. 1993; Al-Kohairy et al. 1994), *S. cerevisiae* (Sanchez et al. 1999), and *Xenopus laevis* (Kumagai et al. 1998) and *grapes* in *D. melanogaster* (Fogarty et al. 1997; Sibon et al. 1997; Su et al. 1999). In *S. cerevisiae*, Chk1 controls the pre-anaphase arrest after DNA damage by preventing degradation of Pds1, an inhibitor of anaphase entry (Sanchez et al. 1999). In *S. pombe* and *Xenopus*, Chk1 is required for the G_2 arrest induced by DNA damage, and in *Xenopus* for the prophase I arrest of oocytes (Nakajo et al. 1999). In *S. pombe*, Chk1 is phosphorylated in response to DNA damage in a Rad3-dependent manner and this is accompanied by an increase in 14-3-3 protein association (Walworth and Benards 1996; Chen et al. 1999). In *D. melanogaster*, *grapes* mutants display an embryonic lethal phenotype similar to that of *mei-41* mutants. Although the phenotype of *mei-41* and *grapes* mutants is complex, at least part of the defects is likely to be attributed to premature entry of mitosis.

Less is known about Chk1 function in mammals. In human cells, Chk1 is shown to be phosphorylated in response to IR and thus, is implicated in the DNA damage response pathway (Sanchez et al. 1997). Because yeast and human Chk1 can phosphorylate Cdc25C in vitro on the inhibitory phosphorylation site S216, Chk1 may function as an effector of the DNA damage checkpoint that activate G_2 arrest by inhibiting Cdc2 kinase activities through Cdc25C. It is currently unclear, however, which PIK members are the regulators of Chk1 in mammalian cells. Thus, we generated a *CHK1* knockout mouse and subsequently, a conditional *CHK1*-deficient ES cell line. Our results indicate that Chk1 is regulated by Atr and plays a crucial role in the G_2/M DNA damage checkpoints, embryonic development, and tumor suppression. A model concerning the mammalian DNA damage response pathway will also be discussed.

Results

Generation of a Chk1 knockout mouse

We disrupted the *CHK1* gene in murine ES cells by gene targeting. The targeting vector consists of a *neo* marker for positive selection flanked by 1.9 kb and 4.5 kb of *CHK1* homologous sequences, and a *TK* marker for negative selection (Fig. 1A). Homologous recombination with this targeting vector removes 3 kb of *CHK1* genomic sequence, including exons 2–5 that encode the putative first methionine, the "G×G××G" ATP-binding motif and half of the kinase domain. Thus, it is likely to generate a null allele. Eight Chk1 heterozygous ES clones were obtained from screening 192 G418- and FIAU-resistant colonies (Fig. 1B). Four independent cell lines were injected to generate chimeras, of which three produced germ-line transmission. The phenotype, as described below, was consistent among all different lines.

Chk1 deficiency results in peri-implantation lethality

CHK1 heterozygous mice are healthy, fertile, and tumor-free up to 1.5 years of age. However, when the heterozygous mice were intercrossed, no *CHK1* homozygous mice were detected among 139 offspring, indicating that Chk1 deficiency results in embryonic lethality. Systematic analysis of embryonic day 6.5 (E6.5)–E15.5 embryos generated from heterozygotes matings failed to detect *CHK1* null embryos at any stage examined (data not shown). Empty decidua and remains of resorbed embryos were often observed at E6.5 or E7.5 in heterozygotes intercross, but were rarely seen in backcross between heterozygous and wild-type mice (Fig. 1C; data not shown). These results suggest that the lethality of *CHK1* null embryos may occur before E6.5.

Therefore, we isolated and cultured blastocysts from intercrossed *CHK1* heterozygous females at E3.5. PCR genotyping of newly isolated blastocysts revealed that the fraction of *CHK1* null embryos was always between one-seventh and one-sixth, well below the predicted one-quarter Mendelian ratio. And these null embryos often displayed abnormal morphology distinctive from their wild-type or heterozygous littermates (data not shown). When these blastocysts were cultured in vitro up to 7 days, the majority would continue to proliferate, hatch from the zona pellucida on the first or second day in culture, and immediately attach or "implant" to the Petri dish surface (Fig. 2A). The trophoectoderm of blastocysts spread into a single cell layer and divided a few times before terminally differentiating into giant trophoblast cells. Above the trophoblast cells lay the inner cell mass (ICM), which continued to proliferate to generate a large cell mass. These proliferating blastocysts, by genotyping, consisted of only wild type and heterozygotes with a 1:2 ratio. In contrast, a small group of blastocysts would stop proliferation, fail to hatch, and degenerate inside the zona pellucida (Fig. 2A). These nonproliferative blastocysts were presumably the missing homozygous mutant embryos, however, their genotype could not be confirmed by PCR due to massive DNA fragmentation during embryo degeneration. Three mutant blastocysts hatched on the third or fourth day in culture, laying down a few trophoblast cells but no ICM. We obtained the genotype of two of these embryos and both were *CHK1*$^{-/-}$. These results suggested that *CHK1*$^{-/-}$

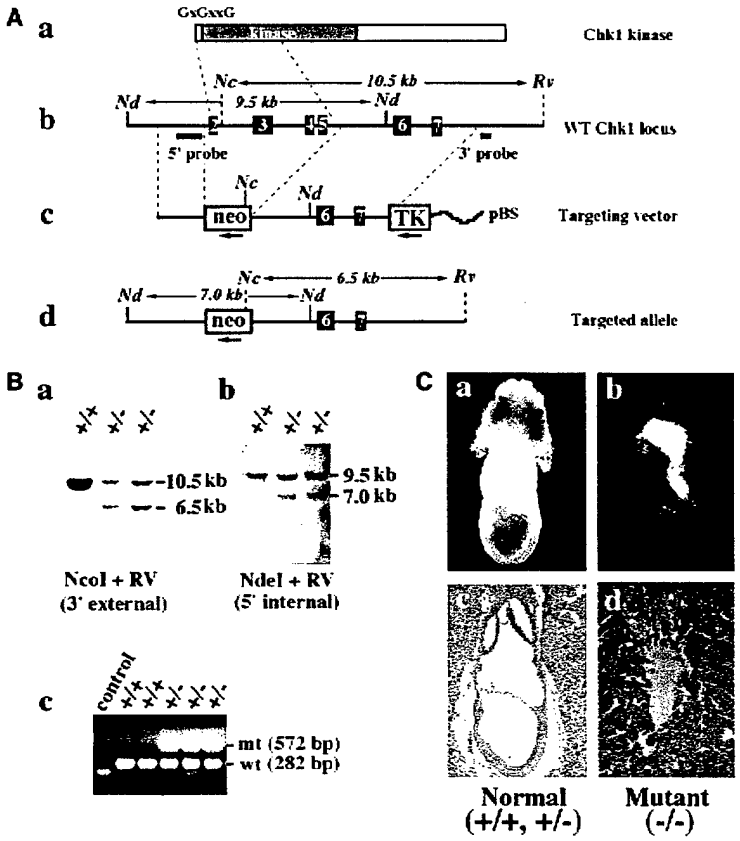

Figure 1. *CHK1* disruption results in early embryonic lethality. (*A*) Disruption of the *CHK1* gene in ES cells. (*a*) Chk1 protein structure. Located at the amino terminus are the "GxGxxG" ATP-binding motif and kinase domain. (*b*) Restriction map of the wild-type *CHK1* locus including exons 2–7 and location of the 3′ external and 5′ internal probes used for Southern blots shown below. (*c*) Restriction map of the *neo* targeting vector. The direction of transcription is shown by arrows beneath the *neo* and *TK* markers. (pBS) pBluescript plasmid. (*d*) Predicted restriction map of the targeted *CHK1* allele. Only relevant restriction sites are shown. (*Nc*) *Nco*I; (*Nd*) *Nde*I; (*Rv*) *Eco*RV. (*B*) Identification of $CHK1^{+/-}$ ES clones by Southern blot analysis. (*a*) Genomic DNA was digested with *Nco*I and *Eco*RV and probed with the 3′ external probe. Genotypes are shown above each lane. $CHK1^{+/-}$ ES clones showed a 10.5-kb wild-type and a 6.5-kb mutant band as predicted. (*b*) Genomic DNA was digested with *Nde*I and probed with the 5′ internal probe. $CHK1^{+/-}$ ES clones displayed a 9.5-kb wild-type and a 7.0-kb mutant band. (*c*) *CHK1* genotyping by PCR. The wild-type and mutant *CHK1* alleles generate a 282-bp and a 572-bp band, respectively. (*C*) Morphological and histological analysis of E7.5 embryos isolated from $CHK1^{+/-}$ intercrosses. A typical photograph is shown for normal (*a,c*) and mutant (*b,d*) E7.5 embryos freshly dissected from decidua (*a,b*) or hematoxylin and eosin-stained sections of E7.5 decidua (*c,d*).

blastocysts have a proliferation defect and that Chk1 may be required for proliferation or survival of early embryonic cells.

Because less than one-quarter of blastocysts were homozygotes and they often displayed abnormal morphology, we examined eight-cell morula isolated from intercrossed $CHK1^{+/-}$ females at E2.5. PCR genotyping revealed the predicted 1:2:1 ratio of $CHK1^{+/+}$:$CHK1^{+/-}$:$CHK1^{-/-}$ embryos at the eight-cell stage (Fig. 2C; data not shown). When these morula were cultured in vitro, it was found that $CHK1^{-/-}$ embryos developed normally until the early blastocyst stage; however, unlike the wild-type and heterozygous littermates, they failed to continue proliferation or hatch and subsequently degenerated inside the zona pellucida (Fig. 2B). These in vitro embryo culture experiments suggest that Chk1 deficiency results in peri-implantation embryonic lethality.

CHK1 deficient embryos die of p53-independent apoptosis

To determine whether *CHK1*-deficient embryos were dying of apoptosis, we isolated eight-cell morula at E2.5 and allowed them to develop in vitro into early stage blastocysts. We then used these blastocysts to perform terminal deoxynucleotide end-labeling (TUNEL) assays that fluorescently labels the ends of fragmented DNA, a hallmark of apoptotic cells. Although wild-type and heterozygous littermates normally showed two to four fluorescent dots, *CHK1* homozygous blastocysts displayed many fluorescent dots, indicative of massive apoptosis (Fig. 2D). To further confirm the TUNEL results, we stained these embryos with 4,6-diamidino-2-phenylindole (DAPI) and observed them under the confocal microscope. Indeed, many cells in $CHK1^{-/-}$ embryos had condensed and fragmented nuclei that is characteristic of apoptosis (Fig. 2E). These results suggest that *CHK1*-deficient embryos die of apoptosis at the blastocyst stage.

To determine whether p53 is responsible for the apoptosis observed in blastocysts, we mated $p53^{-/-}$ $CHK1^{+/-}$ male and female mice, which is expected to generate $p53^{-/-}$ mice with $CHK1^{+/+}$, $CHK1^{+/-}$, and $CHK1^{-/-}$ genotype with a 1:2:1 ratio. Eight-cell morula were isolated from these intercrosses at E2.5, cultured for 2 days and picked for the TUNEL assay. The p53 null mutations could neither rescue nor delay the early lethality of $CHK1^{-/-}$ embryos (data not shown). Furthermore, $CHK1^{-/-}$ $p53^{-/-}$ blastocysts underwent apoptosis to the same degree as $CHK1^{-/-}$ blastocysts, suggesting that the apoptosis is independent of p53.

Chk1 is essential for ES cell viability

To investigate the function of Chk1 at the cellular level, we attempted to generate $CHK1^{-/-}$ ES cells by sequential

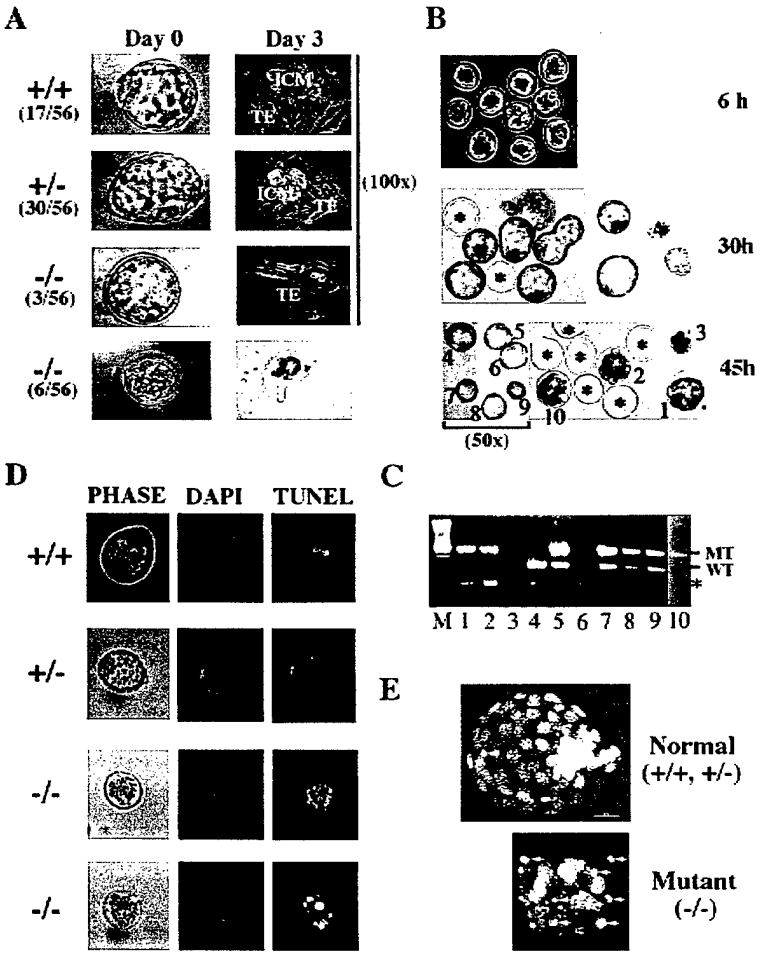

Figure 2. In vitro culture of preimplantation embryos. (*A*) In vitro culture of blastocysts isolated from *CHK1*$^{+/-}$ intercrosses. A typical image at day 0 and day 3 are shown along with the percentage of each category. (TE) Trophoectoderm; (ICM) inner cell mass. All images are 320× except when otherwise indicated. (*B*) In vitro culture of eight-cell morula. Shown here are a litter of 10 embryos isolated from a *CHK1*$^{+/-}$ intercross. The images were captured at 6, 30, and 45 hr in culture (100× except when otherwise indicated). The asterisks indicate the empty zona pellucida after the embryos have hatched. The embryos were individually picked and labeled 1–10. Embryos 1, 2, 3, and 10 failed to hatch. (*C*) PCR genotyping of embryos from *B*. The lane numbers correspond to that of the embryos. Embryo 6 was lost during transfer and embryo 3 was too degenerate to give any products. (WT) Wild type; (MT) mutant. The asterisk indicates a nonspecific band generated by primers alone. (*D*) TUNEL analysis of blastocysts derived as described in *B* (100×). (*E*) Confocal images (DAPI, 1000×) of blastocysts analyzed in *D*. The arrows indicate condensed and fragmented nuclei.

gene targeting. A second targeting vector containing the *hprt* marker was constructed and used to transfect *CHK1*$^{+/-}$ ES cells, in which one *CHK1* allele was disrupted previously by *neo*. When selected for both markers, no targeting event could be obtained from 384 G418/HAT/FIAU-resistant colonies. When selected only for *hprt*, 18 targeted clones were obtained after screening 351 HAT/FIAU-resistant colonies and in all cases the *hprt* construct had replaced the *neo*-disrupted mutant allele instead of the wild-type gene (data not shown). These results suggest that Chk1 is probably essential for proliferation or survival of ES cells.

Therefore, we constructed conditional *CHK1*-deficient ES cells by flanking the second exon of one *CHK1* allele with *loxP* sites and disrupting the other by gene targeting (Fig. 3A,B). This *lox*-flanked (flox) *CHK1* allele can be converted into a null allele after excision of exon 2 by Cre–*lox* site-specific recombination because it contains the translational initiation sequence and encodes the ATP-binding site for the kinase. When three independent *CHK1*$^{flox/-}$ cell lines were transfected transiently with a *CMV:Cre* plasmid, no excised clones were detected by Southern blot analysis among total of ~400 ES colonies (data not shown). However, when a control *CHK1*$^{flox/+}$ cell line was transfected with *CMV:Cre*, 28% (25 of 88) of the colonies underwent 100% excision, whereas an additional 10% (9 of 88) underwent partial or postmitotic excision, generating chimeric colonies (data not shown). These results confirm our prediction that excision of exon 2 from the *CHK1* gene generates a null allele, and are consistent with the previous finding that Chk1 plays an essential role in ES cells. Furthermore, the lack of chimeric excised colonies for Cre-transfected *CHK1*$^{flox/-}$ cells suggests that the defects associated with *CHK1*$^{-/-}$ cells are cell-autonomous and cannot be rescued by mixing with wild-type cells.

The absence of *CHK1*$^{-/-}$ colonies could theoretically be explained by an inability of the *CHK1*$^{flox/-}$ cells to excise or by cell death after the excision. To distinguish these two possibilities, we transfected both *CHK1*$^{flox/+}$ and *CHK1*$^{flox/-}$ ES cells with a *PGK:Cre* plasmid by electroporation and harvested cells after 24, 48, 72, and 96 hr. Southern blot analysis revealed that *CHK1*$^{flox/-}$ cells underwent excision as efficiently as *CHK1*$^{flox/+}$ cells (Fig. 3C, cf. lanes 2,3 with lanes 6,7). The excised and nonexcised cells were represented by the 7.5-kb and 5.1-kb band, respectively. Judging by their relative intensities, we estimated that ~60%–70% of cells underwent flox

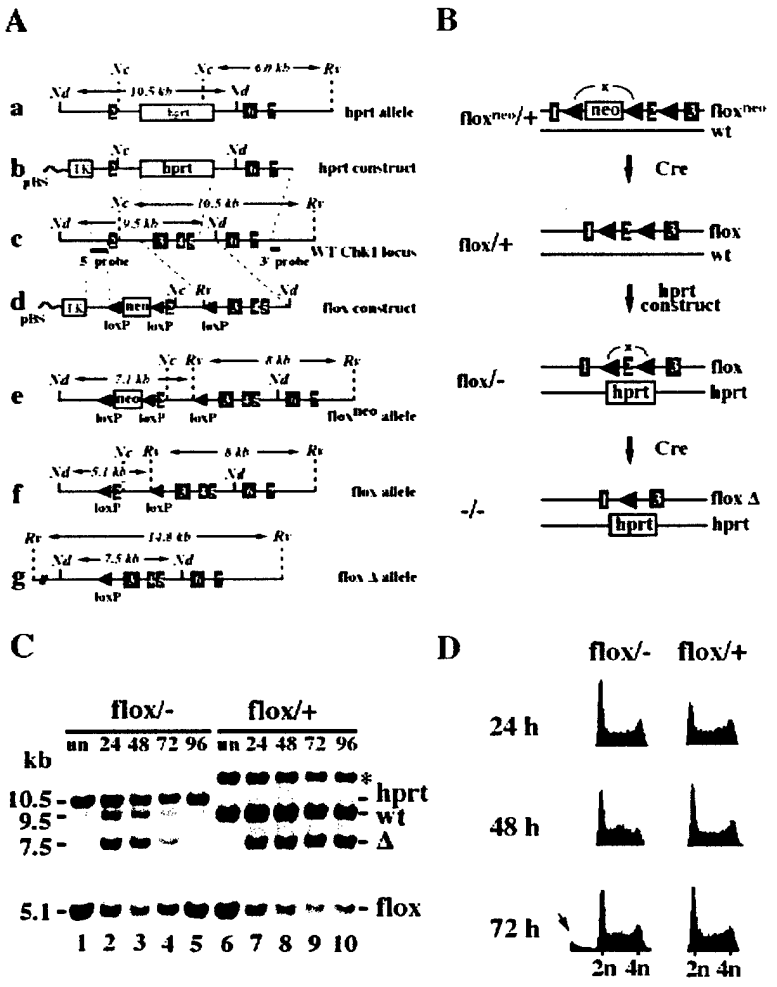

Figure 3. Construction and analysis of a conditional *CHK1*-deficient ES cell line. (*A*) Restriction maps of targeting vectors and targeted alleles. (*a*) *hprt* targeted allele; (*b*) *hprt* targeting vector; (*c*) wild-type *CHK1* locus; (*d*) flox targeting vector; (*e*) flox^{neo}-targeted allele; (*f*) flox allele generated after *neo* excision; (*g*) flox Δ allele generated after excision of exon 2. Only relevant restriction sites are shown. (*Nc*) *Nco*I; (*Nd*) *Nde*I; (*Rv*) *Eco*RV. (*B*) A schematic representation of the construction of conditional *CHK1*-deficient ES cells. In brief, a *CHK1* flox^{neo}/+ cell line was first obtained using the flox-targeting vector followed by the Cre–*lox*P-mediated *neo* excision to create *CHK1*$^{flox/+}$ cells. The remaining wild-type gene was then disrupted in the *CHK1*$^{flox/+}$ cells by the *hprt* targeting vector to generate *CHK1*$^{flox/-}$ cells. Finally, *CHK1*$^{flox/-}$ cells were conditionally converted into *CHK1*$^{-/-}$ cells by excision of exon 2 by transient transfection of *PGK:Cre*. (*C*) A Southern blot showing excision of the flox allele in *CHK1*$^{flox/+}$ and *CHK1*$^{flox/-}$ cells. Both are sister cell lines obtained from the same screen for generating *CHK1*$^{flox/-}$ cells. The asterisk refers to a band produced by random integration of the *hprt* construct in the *CHK1*$^{flox/+}$ cells. Genomic DNA was prepared from untransfected (lanes *1,6*) or Cre-transfected cells (lanes *2–5* and *7–10*) collected at 24, 48, 72, and 96 hr after electroporation, digested with *Nde*I and *Eco*RV and probed with the 5′ internal probe. Δ refers to the excised flox allele. The faint wild-type band present in lanes *2–4* was contributed by the feeder cells. (*D*) Comparison of Cre-transfected *CHK1*$^{flox/+}$ and *CHK1*$^{flox/-}$ cells by FACS (DNA content) analysis. Cells were harvested at 24, 48, and 72 hr after electroporation and stained with propidium iodide (PI). The arrow indicates cells with less than 2N DNA content that were present in the 72-hr flox/- sample.

excision in both cell lines by 48 hr after Cre transfection (Fig. 3C, lanes 3,8). However, although the excised flox/+ cells divided as fast as the nonexcised cells, the excised flox/- cells disappeared from the culture between 72 and 96 hr (Fig. 3C, cf. lanes 4,5 and lanes 9,10). Analysis of DNA content by FACS revealed a significant sub-G_1 population, which is characteristic of apoptotic cells, in the Cre-transfected *CHK1*$^{flox/-}$ cells at 72 hr after transfection (Fig. 3D). These results indicate that *CHK1*$^{-/-}$ cells have a severe proliferation defect accompanied by apoptotic death.

CHK1$^{-/-}$ *cells are defective for the* G_2*/M DNA damage checkpoint*

IR induces a predominant G_2 arrest in mouse ES cells (Aladjem et al. 1998; Hirao et al. 2000). To determine whether Chk1 is required for this G_2 arrest, we subjected *CHK1*$^{flox/-}$ ES cells to 10 Gy of IR at 24 hr after transfection with a *PGK:Cre* or a *CMV:GFP* plasmid. Twelve hours after irradiation, ~70%–80% of all cell types arrested at G_2 with a 4N DNA content, as measured by FACS analysis (Fig. 4A). However, at later time points the G_2-arrested population of *CHK1*$^{flox/-}$ cells declined, whereas the G_1–S population increased to 43.7% (18 hr) and 53.9% (24 hr), as more cells were converted to *CHK1*$^{-/-}$ cells (Fig. 4A). In contrast, all the control cells remained predominantly arrested at G_2. These results suggest that *CHK1*$^{-/-}$ cells may lack a functional G_2/M DNA damage checkpoint.

To determine whether *CHK1*$^{-/-}$ cells enter mitosis in the presence of DNA damage, we took advantage of the fact that mouse ES cells have a functional spindle checkpoint (Hirao et al. 2000). Cells were irradiated as described above and immediately placed in media containing nocodazole that will disrupt spindles and trigger a mitotic arrest. Twelve hours after IR and nocodazole treatment, 90% of all cell types arrested with a 4N DNA

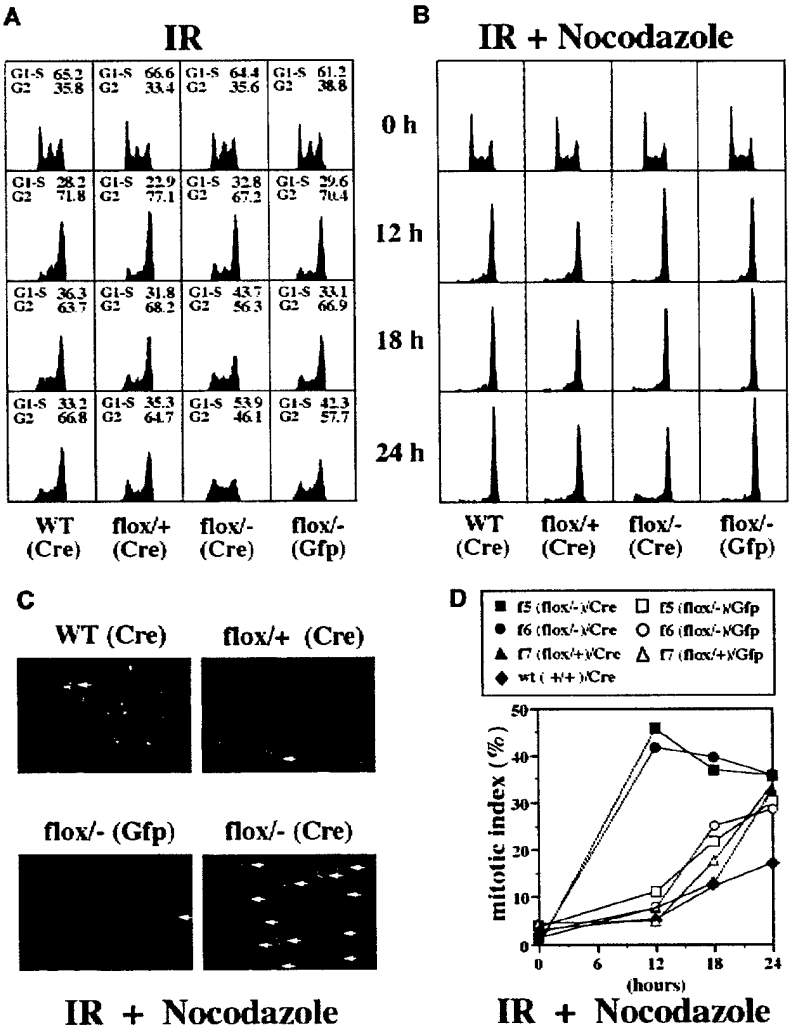

Figure 4. *CHK1*$^{-/-}$ cells are defective for the G_2/M DNA damage checkpoint. (*A*) FACS (DNA content) analysis of irradiated GFP- or Cre-transfected *CHK1*$^{+/+}$, *CHK1*$^{flox/+}$, and *CHK1*$^{flox/-}$ cells. Twenty-four hours after transfection, cells were subjected to 10 Gy IR, harvested at 0, 12, 18, and 24 hr and stained with PI. The percentage of G_1–S and G_2 population (mitotic cells are included in the G_2 counts but are generally a small proportion) is shown above each FACS sample. (*B*) FACS (DNA content) analysis of IR and nocodazole-treated cells. Cells of the indicated genotypes were transfected and irradiated as in *A* and incubated in nocodazole (0.2 μg/ml) containing media 30 min after irradiation. (*C*) Images (1000×) of the DAPI-stained 12-hr samples in *B*. Arrows indicate mitotic cells with condensed chromosomes and no nuclear membrane. (*D*) A mitotic index graph of IR and nocodazole-treated cells described in *B* and *C*. Cells (250–300) were counted for each sample. GFP or Cre transfections are indicated by open or closed circles. f5 and f6 represent two independent *CHK1*$^{flox/-}$ cell lines and f7 is a control *CHK1*$^{flox/+}$ cell line.

content as measured by FACS analysis (Fig. 4B). However, 40%–45% of Cre-transfected *CHK1*$^{flox/-}$ cells entered mitosis, in contrast to only 5%–8% of mitotic cells in GFP-transfected *CHK1*$^{flox/-}$ cells or Cre-transfected *CHK1*$^{+/+}$ and *CHK1*$^{flox/+}$ control cells (Fig. 4C,D). Because 60%–70% of *CHK1*$^{flox/-}$ cells are converted into *CHK1*$^{-/-}$ cells after *PGK:Cre* transfection, we estimate that at least 60% of *CHK1*$^{-/-}$ cells prematurely enter mitosis in spite of DNA damage. Thus, Chk1 is a bona fide component of the mammalian G_2/M DNA damage checkpoint. Furthermore, in response to DNA damage, the rapid kinetics and degree of inappropriate mitotic entry for *CHK1*$^{-/-}$ cells suggest that Chk1 is required for the initiation of G_2 arrest in response to DNA damage.

CHK1 *heterozygosity modestly enhances tumorigenesis of* WNT-1 *transgenic mice*

Examination of *CHK1*$^{+/-}$ animals up to the age of 18 months failed to detect a predisposition to early tumorigenesis. To determine whether reduction of *CHK1* dosage could enhance tumor formation in the context of other oncogenic stimuli, we crossed *CHK1*$^{+/-}$ mice to *WNT-1* transgenic mice, which contain a *WNT-1* oncogene driven by a mammary gland-specific mouse mammary tumor virus promoter (Tsukamoto et al. 1988). The *WNT-1* transgenic females develop early mammary gland hyperplasia and subsequent mammary adenocarcinomas at the ages of 3–12 months. Previous crosses of p53- and p21-deficient mice to *WNT-1* transgenic mice have revealed synergistic enhancements of tumor incidence or tumor growth rates in the bitransgenic offspring (Donehower et al. 1995; Jones et al. 1999). After the *WNT-1* transgenic/*CHK1*$^{+/-}$ crosses, we monitored 22 *CHK1*$^{+/-}$ *WNT-1* transgenic females and 22 *CHK1*$^{+/+}$ *WNT-1* transgenic females for tumors of the mammary gland. *CHK1*$^{+/-}$ females showed an earlier onset of mammary tumors compared to the *CHK1*$^{+/+}$ females (Fig. 5). The average age of tumor formation in the *CHK1*$^{+/-}$ mice was 168 days versus 219 days for *CHK1*$^{+/+}$ mice.

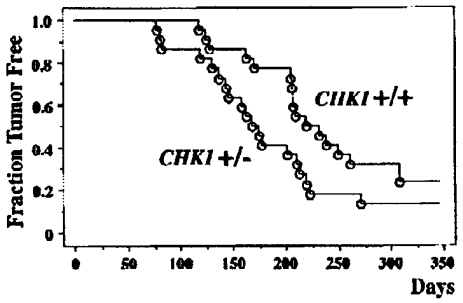

Figure 5. Kaplan-Meier plot of tumor incidence in *CHK1*$^{+/+}$ and *CHK1*$^{+/-}$ *WNT-1* transgenic females. Twenty-two animals of each genotype were monitored for mammary tumor formation for ~10 months. Tumor-free survival is plotted against the animal age in days.

Statistical comparison of the tumor incidence curves by the log-rank test, the Breslow-Gehan-Wilcoxon test, and the Peto-Peto-Wilcoxon test gave P values of 0.055, 0.030, and 0.030, respectively. These test scores indicate that the differences in tumor incidence between the *CHK1*$^{+/+}$ and *CHK1*$^{+/-}$ mice are marginally significant at the 0.05 level.

Further comparison of the *CHK1*$^{+/+}$ and *CHK1*$^{+/-}$ mammary adenocarcinomas revealed no obvious differences in gross pathology, histopathology, or growth rates. To assess whether the remaining wild-type *CHK1* allele was lost in the *CHK1*$^{+/-}$ tumors, we analyzed genomic DNA isolated from *CHK1*$^{+/-}$ tumors by Southern blot analysis. Of nine tumors examined, all nine retained an intact wild-type *CHK1* allele (data not shown), suggesting that reduction of *CHK1* dosage by 50% has a modest tumor-enhancing effect in the *WNT-1* transgenic model. The retention of the wild-type *CHK1* allele in the tumors is consistent with the finding that complete absence of Chk1 protein leads to cell lethality.

In vivo phosphorylation of Chk1 on S345 by Atr after DNA damage

In human cells, Chk1 is phosphorylated in response to DNA damage (Sanchez et al. 1997). Because SQ sites are known substrates of Atm and Atr (Banin et al. 1998; Canman et al. 1998), we raised rabbit polyclonal antibodies to peptides containing phosphorylated serine in the conserved SQ sites in human Chk1 protein. Only the anti-phospho-S345 (anti-p-S345) antibodies produced a signal specific for the phospho–antigen-peptide. Chk1 was immunoprecipitated with anti-Chk1 or anti-p-S345 antibodies from lysates prepared from 293T cells that were either untreated or treated with hydroxyurea (HU), UV, or IR. Although the anti-Chk1 antibodies brought down equivalent amounts of Chk1 proteins from all cell lysates, the anti-p-S345 antibodies immunoprecipitated Chk1 proteins only from HU-, UV-, or IR-treated cells, but not from untreated cells (Fig. 6A). This experiment suggests that in human cells Chk1 is phosphorylated on S345 in response to DNA damage or replication blocks.

Because *ATR* and *CHK1* disruptions both lead to peri-implantation embryonic lethality in mice, we asked whether Atr regulates Chk1 in response to DNA damage. By transient transfection experiments, we showed that overexpression of wild-type Atr, but not the kinase-defective mutant Atr, increases the phosphorylation of co-transfected Chk1 on S345 in response to UV (Fig. 6B). Furthermore, overexpression of the kinase-defective mutant Atr in an inducible cell line (Cliby et al. 1998) inhibits the UV-induced S345 phosphorylation of endogenous Chk1 (Fig. 6C). These results suggest that Atr functions upstream of Chk1 in the mammalian DNA damage response pathway and is a major regulator of Chk1 phosphorylation after DNA damage.

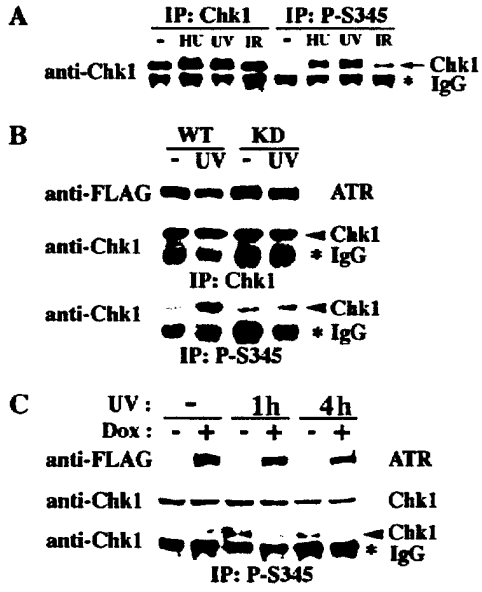

Figure 6. Chk1 is phosphorylated on S345 after DNA damage and this is regulated by Atr. (*A*) Phosphorylation of Chk1 on S345 after DNA damage. 293T cells were untreated or treated with IR (20 Gy and harvested after 1 hr), UV (50 J/m^2 and harvested after 2 hr) or HU (1 mM for 24 hr). Whole cell lysates were immunoprecipitated (IP) with rabbit anti-Chk1 or anti-p-S345 antibodies followed by immunoblotting with mouse anti-Chk1 antibodies. (*B*) Overexpression of wild-type (WT) but not kinase-deficient (KD) Atr enhances S345 phosphorylation of cotransfected Chk1. Thirty-six hours after cotransfection of *CMV:Chk1* and *CMV:FLAG-Atr–WT* or *CMV–FLAG–Atr–KD*, 293T cells were untreated (–) or treated with UV (50 J/m^2) and harvested after 1.5 hr. Whole cell lysates were immunoblotted with anti-FLAG antibodies to detect Atr expression, or assayed for S345 phosphorylation of Chk1 by IP–Western blot as described in (*A*). (*C*) Induction of kinase-deficient Atr inhibits S345 phosphorylation of endogenous Chk1. GM847/ATR–KD cells were cultured in the absence (–) or presence (+) of 1 μg/ml doxycycline (Dox) for 48 hr, untreated (–) or treated with UV (50 J/m^2) and harvested after 1 (1h) or 4 (4h) hr. Whole cell lysates were immunoblotted with anti-FLAG or mouse anti-Chk1 antibodies to detect Atr–KD or endogenous Chk1 expression. And IP–Western was performed to detect S345 phosphorylation of Chk1 as described in *A*.

Discussion

Chk1 is essential for embryonic development and ES cell survival

CHK1 deficiency leads to cell death in ES cells and periimplantation embryonic lethality in mice. Thus, the early lethality of *CHK1* null embryos can be explained by a cell autonomous failure of $CHK1^{-/-}$ embryonic cells to survive. Given the essential role of Chk1 in each cell cycle, it is surprising that *CHK1* null embryos can survive even to the blastocyst stage. A few embryonic divisions may be sustained in the *CHK1* null embryos by maternal Chk1 protein stores. Alternatively, $CHK1^{-/-}$ embryonic cells may be capable of dividing a few times before apoptotic death. Regulated apoptosis occurs in wild-type murine blastocysts and is thought to eliminate redundant or damaged cells before implantation to ensure successful embryonic development (Parchment 1991). Thus, the massive apoptosis displayed by *CHK1* null blastocysts may indicate that $CHK1^{-/-}$ cells accumulate substantial genomic instability. The fact that apoptosis occurs independent of p53 in wild-type and *CHK1* mutant blastocysts is consistent with the previous finding that ES cells undergo p53-independent apoptosis in response to DNA damage (Aladjem et al. 1998).

Although required for DNA damage checkpoints, *CHK1* is not an essential gene in yeast *S. cerevisiae* or *S. pombe*. In contrast, Grapes/Chk1 is indispensable for early embryonic development in fruit flies and, as shown here, in mice. It remains unclear whether this embryonic lethality is due to the cell cycle checkpoint function of Chk1, or to some novel function acquired in evolution. It is known, however, that embryonic development is extremely sensitive to genomic instability. Consistently, disruption of many genes involved in double-stranded DNA break repair, including BRCA1, BRCA2, RAD50, RAD51, and MRE11, lead to early embryonic lethality in mice. Many of these genes have also been shown to be essential for ES cell viability and chromosomal stability (Hakem et al. 1996; Lim and Hasty 1996; Sharan et al. 1997; Luo et al. 1999; Yamaguchi-Iwai et al. 1999). Thus, if Chk1 mutant cells are checkpoint defective and cannot fully repair DNA damage during normal cell cycle, it might lead to the accumulation of genomic instability, cell death, and embryonic lethality.

CHK1 *and* ATR *may define a new class of tumor suppressors*

Given the degree of genomic instability seen in $ATR^{-/-}$ cells and possibly $CHK1^{-/-}$ cells, *CHK1* and *ATR* are likely to be potent tumor suppressor genes. *ATR* heterozygotes have a small increase in tumor incidence (Brown and Baltimore 2000), whereas *CHK1* heterozygosity modestly enhances the tumorgenicity of *WNT-1* oncogenic mice. A limited analysis failed to detect any incidence of loss of heterozygosity (LOH) in $ATR^{+/-}$ or $CHK1^{+/-}$ tumors. This is consistent with the fact that complete absence of these proteins leads to cell lethality. Likewise, increase in spontaneous or carcinogen-induced tumor formation has been observed in p27 heterozygotes and some p53 heterozygotes without LOH (Fero et al. 1998; Venkatachalam et al. 1998). Because *ATR* and *CHK1* are both essential genes that in the heterozygous state can modestly enhance tumorigenesis, they may represent a novel class of essential tumor suppressor genes that fail to display LOH in developing tumors. This also suggests that not all tumor suppressor genes can be detected by simply searching for mutations in the remaining allele of genes within a particular region of LOH. Thus, it might be prudent to give careful consideration to those genes believed to be essential for viability as important candidates for tumor suppressor genes.

Chk1 is required for initiating G_2 arrest after γ-irradiation

In response to IR, mouse ES cells arrest predominantly at G_2 and Chk2 is required to maintain this arrest (Hirao et al. 2000). Similarily, p53, p21, and 14-3-3 sigma have been shown to help sustain the IR-induced G_2 arrest in human fibroblast cells (Bunz et al. 1998; Chan et al. 1999). Our analysis of the conditional *CHK1*-deficient ES cells indicates that Chk1 is primarily responsible for the initiation of G_2 arrest in response to DNA damage. Chk1 and Chk2 have been shown to phosphorylate human Cdc25C on S216 in vitro (Furnari et al. 1997; Sanchez et al. 1997; Matsuoka et al. 1998; Blasina et al. 1999; Brown et al. 1999; Chaturvedi et al. 1999). S216 phosphorylation of Cdc25C is important for G_2 arrest after DNA damage (Peng et al. 1997) because it causes inhibition and cytoplasmic sequestration of Cdc25C, thereby preventing the activation of Cdc2 kinase (Kumagai and Dunphy 1999; Lopez-Girona et al. 1999; Yang et al. 1999). Because the S216 site is not conserved in mouse Cdc25C, other similarly acting phosphorylation sites may exist as targets of these checkpoint kinases. Furthermore, it is likely that additional targets for Chk1 and Chk2 also contribute to cell cycle arrest (O'Connell et al. 1997). Our results are consistent with the model in which Chk1 primarily functions to initiate the G_2 arrest in response to DNA damage and Chk2 plays a supporting role in maintaining this arrest both by preventing the activation of Cdc2 kinase through Cdc25C. Because mouse ES cells have an unusual cell cycle, it will be important to study Chk1 and Chk2 function in DNA damage checkpoints in other cell types.

Chk1 is modified in response to DNA damage

In yeast and humans, Chk1 is phosphorylated in response to DNA damage (Walworth et al. 1993; Sanchez et al. 1997, 1999). The phosphorylation of human Chk1 can only be reliably detected by two-dimensional gel analysis. To establish a simpler assay for Chk1 activation, we made phospho-specific antibodies and found that anti-p-S345 antibodies were able to immunoprecipitate Chk1 efficiently only when cells were treated with DNA-damaging or replication-interfering agents such as UV and HU, and to a lesser extent with IR. Analysis of

Chk1 phosphorylation was complicated by the fact that it runs on a gel at a position obscured by the heavy chain of IgG. The assay we used could not distinguish regulated phosphorylation of Chk1 on S345 versus constitutive phosphorylation with regulated accessibility by antibodies. However, given the knowledge of Chk1 phosphorylation in other systems, we favor the idea that human Chk1 is phosphorylated on S345 in response to DNA damage or replication blocks. The S345 site ISF-(pS)QP is very similar to the consensus 14-3-3 binding sequence RSx(pS)xP, suggesting that phosphorylated human Chk1 protein may interact with 14-3-3 proteins. Phosphorylation of this conserved site in *S. pombe* Chk1 could potentially explain the increase in 14-3-3 binding to Chk1 after DNA damage (Chen et al. 1999).

Atr regulates Chk1

Both Atr/Mei-41 and Chk1/Grapes are required for early embryogenesis in mice and fruit flies, suggesting Atr and Chk1 function in the same pathway. We propose that Atr is a major regulator of Chk1 in response to DNA damage based on the following observations: (1) Chk1 phosphorylation on S345 is increased in response to UV and HU treatment, to which cells expressing kinase-defective mutant Atr show enhanced sensitivity (Cliby et al. 1998); (2) overexpression of Atr enhances Chk1 S345 phosphorylation in response to UV; (3) Atr can phosphorylate the S345 site in vitro when presented as a GST fusion peptide (Kim et al. 1999); (4) overexpression of the kinase-defective mutant Atr reduces S345 phosphorylation of endogenous Chk1 in response to UV; and (5) like *CHK1*$^{-/-}$ cells, cells expressing the kinase-defective mutant Atr are compromised for the IR-induced G_2 arrest (Cliby et al. 1998). Taken together, these results suggest that Atr functions upstream of Chk1 and regulate its phosphorylation on S345 in response to DNA damage.

Our results are consistent with a model shown in Figure 7, in which Atm–Chk2 and Atr–Chk1 represent two parallel branches in the mammalian DNA damage response pathway that respond primarily toward different types of DNA damage. Atm responds primarily to DNA-damaging agents that cause double-stranded breaks, such as IR, and phosphorylates Chk2. Atm and Chk2 together phosphorylate Brca1 and p53 (Banin et al. 1998; Canman et al. 1998; Cortez et al. 1999; Chehab et al. 2000; Hirao et al. 2000; Shieh et al. 2000), and activate cellular responses including G_1 arrest. On the other hand, Atr responds primarily to agents like UV and HU that can potentially interfere with DNA replication, and phosphorylates Chk1. It is possible that Atr and Chk1 phosphorylate Brca1, p53 in addition to Cdc25C (Tibbetts et al. 1999; Shieh et al. 2000; R.S. Tibbetts et al., in prep.), and activate cellular responses including G_2 arrest. Furthermore, the two pathways have significant overlap and often cooperate with each other to ensure prompt and efficient repair of DNA damage and to maintain genomic integrity. When one pathway is genetically compromised, they can also function redundantly, although probably to a lesser extent and with different kinetics. For example, the rapid p53 stabilization in response to IR is greatly reduced in *ATM* mutant cells (Kastan et al. 1992), but it does occur much later, which is probably due to Atr (Lu and Lane 1993; Tibbetts et al. 1999). Similar observations have been made for Chk2 phosphorylation in response to IR (S. Matsuoka and S.J. Elledge, unpubl.). This may reflect the fact that in addition to tailoring the cellular response to different types of DNA damage, cells have many responses that are commonly required toward different types of genotoxic stress.

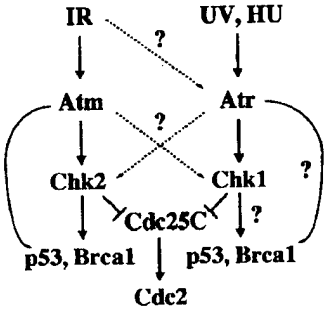

Figure 7. A model for the mammalian DNA damage response pathway (See text for details). The question marks indicate hypothetical regulatory interactions.

Materials and methods

Construction of targeting vectors

All targeting vectors were constructed for positive–negative selection and thus contain a *neo* or *hprt* marker and a *TK* marker. For simplification, we describe the composition of each vector rather than details of construction. *Neo*-targeting vector (pQL258): The *neo* marker was flanked by 1.9 kb of the 5′ untranslated region and 4.5 kb of genomic sequence containing exons 6–7. Hprt-targeting vector (pQL289): The *hprt* marker was flanked by 3 kb of 5′ genomic sequence with exon 2 and 4.2 kb of 3′ genomic sequence with exons 6–7. Flox targeting vector (pQL456): The *lox*P–*neo*–*lox*P cassette was ligated to a 2.2-kb exon 2-containing genomic sequence, of which the last 59 bp was replaced by an *Eco*RV and a *lox*P site. The *lox*P–*neo*–*lox*P–E2–*Rv*–*lox*P centerpiece was flanked by 1.9 kb of 5′ untranslated region and 4.3 kb of 3′ genomic sequence carrying exons 3–5.

Southern blot and PCR

Genomic DNA was isolated from ES cells or mouse tissues using standard protocols and Southern blot analysis were performed with QuikHyb solution (Stratagene). The 3′ external probe was a 420-bp *Hin*dIII–*Nhe*I fragment from pQL253, whereas the 5′ internal probe was a 1.4-kb *Eco*RI–*Xho*I fragment from pQL286. *WNT-1* and p53 genotyping was performed as described (Tsukamoto et al. 1988; Donehower et al. 1992). Preimplantation embryos were digested at 55°C overnight in lysis buffer [10 mM Tris (pH 7.5), 10 mM EDTA (pH 8), 10 mM NaCl, 0.5% Sarcosyl, 0.5 mg/ml protease K] and 1–5 µl lysate was used for PCR. *CHK1* PCR was conducted in 25 µl reaction using Expand DNA polymerase (Boehringer Mannheim) and three primers: 247, 5′-ACCGCTTCCTCGTGCTTTAC-3′; 248, 5′-ATAGGCACCTTCTCCCAAAG-3′; and 252, 5′-GGAGGA-

CAAACGTGGAAACAGG-3'. PCR cycles: 94°C, 3 min, 33 cycles of (94°C, 20 sec; 63°C, 60 sec), 68°C, 4 min. A 282-bp and a 572-bp fragment were amplified from the wild type (by 248 and 252) and mutant alleles (by 247 and 252), respectively.

Manipulations of pre-implantation embryos

All embryos were generated by natural matings. Eight-cell morula were cultured in KSOM media (Cell and Molecular Technologies) and blastocysts in M15 media. All images of in vitro cultured embryos were taken on an inverted microscope using the National Institutes of Health (NIH) imaging software.

TUNEL analysis of blastocysts

Eight-cell morula were isolated, cultured for 45 hr and harvested for TUNEL analysis according to manufacture's protocol (Boehringer Mannheim). In brief, embryos were fixed in 10% formalin for 20 min, permeablized in 0.2% Triton X-100 for 5 min, followed by TUNEL labeling at 37°C for 1 hr and DAPI staining. Stained embryos were individually suspended in PBS solution for imaging on a Zeiss fluorescence microscope. Mutant and normal-looking embryos were divided into two groups: half for genotyping and half mounted for confocal imaging. Normal ($CHK1^{+/+}$ and $CHK1^{+/-}$) versus mutant ($CHK1^{-/-}$) embryos were identified with ~95% confidence.

FACS and mitotic index

FACS analysis was performed with standard protocols. Feeder cells were excluded based on their giant size and greater than 4N DNA content. The percentage of G_1–S and G_2 population was measured by the Coulter (II) software (Beckman). For mitotic index measurement, cells were cytospinned onto slides, fixed in 3% paraformaldehyde for 15 min, permeablized in 0.5% NP40 for 5 min, and mounted in Vectashield containing DAPI (Vector Lab). Feeder cells were excluded based on their giant size and multinuclei.

Antibodies

Mouse anti-FLAG (M5) (Sigma) and anti-Chk1 (Santa Cruz) antibodies were purchased and rabbit anti-(human) Chk1 antibodies were described in Sanchez et al. (1997). The anti-p-S345 antibodies were raised against a human Chk1 phospho-S345 peptide, QGISF(pS)QPTC, and were affinity-purified by the phospho–antigen-peptide column followed by passing through a QGISFSQPTC peptide column to eliminate nonspecific antibodies reacting with the unphosphorylated antigen peptide. Cell lysates were prepared and immunoprecipitation (IP) were performed as described (Matsuoka et al. 1998). IP with anti-p-S345 antibodies was conducted in the presence of 100 μg/ml of the QGISFSQPTC peptide. Immunoblots were visualized by ECL (Amersham).

Acknowledgments

We thank Drs. Yolonda Sanchez, Stephen H. Friend, Karlene A. Cimprich, Philippe Soriano, and Richard Behringer for useful plasmids and reagents, Janet C. Thompson, Louise A. Stanley, and Jessica Wang for technical assistance. We also thank Dr. Michael A. Mancini for generous help on confocal imaging, Drs. Pauline Ward and Zhengzheng Shi for technical advice on manipulation of preimplantation embryos, and Hua Chang, Drs. Tony Carr, Nancy Walworth, Eric Brown, William Sullivan, Anthony Lau, and Pumin Zhang for helpful discussions. X.C. is supported by Karolinska Institute (Sweden)/BCM exchange program and the U.S. Army Breast Cancer Research program. L.A.D. is the recipient of a U.S. Army Breast Cancer Research Program academic award. This work was also supported by NIH grants awarded to S.J.E. and A.B. Both are investigators with the Howard Hughes Medical Institute.

The publication costs of this article were defrayed in part by payment of page charges. This article must therefore be hereby marked "advertisement" in accordance with 18 USC section 1734 solely to indicate this fact.

References

Aladjem, M.I., B.T. Spike, L.W. Rodewald, T.J. Hope, M. Klemm, R. Jaenisch, and G.M. Wahl. 1998. ES cells do not activate p53-dependent stress responses and undergo p53-independent apoptosis in response to DNA damage. *Curr. Biol.* **8:** 145–155.

Al-Khodairy, F., E. Fotou, K.S. Sheldrick, D.J. Griffiths, A.R. Lehmann, and A.M. Carr. 1994. Identification and characterization of new elements involved in checkpoint and feedback controls in fission yeast. *Mol. Biol. Cell.* **5:** 147–160.

Banin, S., L. Moyal, S. Shieh, Y. Taya, C.W. Anderson, L. Chessa, N.I. Smorodinsky, C. Prives, Y. Reiss, Y. Shiloh et al. 1998. Enhanced phosphorylation of p53 by ATM in response to DNA damage. *Science* **281:** 1674–1677.

Barlow, C., S. Hirotsune, R. Paylor, M. Liyanage, M. Eckhaus, F. Collins, Y. Shiloh, J.N. Crawley, T. Ried, D. Tagle et al. 1996. Atm-deficient mice: A paradigm of ataxia telangiectasia. *Cell* **86:** 159–171.

Blasina, A., D. Weyer IV, M.C. Laus, W.H. Luyten, A.E. Parker, and C.H. McGowan. 1999. A human homologue of the checkpoint kinase Cds1 directly inhibits Cdc25 phosphatase. *Curr. Biol.* **9:** 1–10.

Boddy, M.N., B. Furnari, O. Mondesert, and P. Russell. 1998. Replication checkpoint enforced by kinases Cds1 and Chk1. *Science* **280:** 909–912.

Brown, A.L., C.H. Lee, J.K. Schwarz, N. Mitiku, H. Piwnica-Worms, and J.H. Chung. 1999. A human Cds1-related kinase that functions downstream of ATM protein in the cellular response to DNA damage. *Proc. Natl. Acad. Sci.* **96:** 3745–3750.

Brown, E.J. and D. Baltimore. 2000. ATR disruption leads to chromosomal fragmentation and early embryonic lethality. *Genes & Dev.* **14:** 397–402.

Bunz, F., A. Dutriaux, C. Lengauer, T. Waldman, S. Zhou, J.P. Brown, J.M. Sedivy, K.W. Kinzler, and B. Vogelstein. 1998. Requirement for p53 and p21 to sustain G2 arrest after DNA damage. *Science* **282:** 1497–1501.

Canman, C.E., D.S. Lim, K.A. Cimprich, Y. Taya, K. Tamai, K. Sakaguchi, E. Appella, M. B. Kastan, and J.D. Siliciano. 1998. Activation of the ATM kinase by ionizing radiation and phosphorylation of p53. *Science* **281:** 1677–1679.

Chan, T.A., H. Hermeking, C. Lengauer, K.W. Kinzler, and B. Vogelstein. 1999. 14-3-3Sigma is required to prevent mitotic catastrophe after DNA damage. *Nature* **401:** 616–620.

Chaturvedi, P., W.K. Eng, Y. Zhu, M.R. Mattern, R. Mishra, M.R. Hurle, X. Zhang, R.S. Annan, Q. Lu, L.F. Faucette et al. 1999. Mammalian Chk2 is a downstream effector of the ATM-dependent DNA damage checkpoint pathway. *Oncogene* **18:** 4047–4054.

Chehab, N.H., A. Malikzay, M. Appel, and T.D. Halazonetis. 2000. Chk2/hCds1 functions as a DNA damage checkpoint in G(1) by stabilizing p53. *Genes & Dev.* **14:** 278–288.

Chen, L., T.H. Liu, and N.C. Walworth. 1999. Association of Chk1 with 14-3-3 proteins is stimulated by DNA damage. *Genes & Dev.* **13:** 675–685.

Cimprich, K.A., T.B. Shin, C.T. Keith, and S.L. Schreiber. 1996. cDNA cloning and gene mapping of a candidate human cell cycle checkpoint protein. *Proc. Natl. Acad. Sci.* **93:** 2850–2855.

Cliby, W.A., C.J. Roberts, K.A. Cimprich, C.M. Stringer, J.R. Lamb, S.L. Schreiber, and S.H. Friend. 1998. Overexpression of a kinase-inactive ATR protein causes sensitivity to DNA-damaging agents and defects in cell cycle checkpoints. *EMBO J.* **17:** 159–169.

Cortez, D., Y. Wang, J. Qin, and S.J. Elledge. 1999. Requirement of ATM-dependent phosphorylation of Brca1 in the DNA damage response to double-strand breaks. *Science* **286:** 1162–1166.

Donehower, L.A., M. Harvey, B.L. Slagle, M.J. McArthur, C.A. Montgonery Jr., J.S. Butel, and A. Bradley. 1992. Mice deficient for p53 are developmentally normal but susceptible to spontaneous tumors. *Nature* **356:** 215–221.

Donehower, L.A., L.A. Godley, C.M. Aldaz, R. Pyle, Y.P. Shi, D. Pinkel, J. Gray, A. Bradley, D. Medina, and H.E. Varmus. 1995. Deficiency of p53 accelerates mammary tumorigenesis in Wnt-1 transgenic mice and promotes chromosomal instability. *Genes & Dev.* **9:** 882–895.

Elledge, S.J. 1996. Cell cycle checkpoints: Preventing an identity crisis. *Science* **274:** 1664–1672.

Fero, M.L., E. Randel, K.E. Gurley, J.M. Roberts, and C.J. Kemp. 1998. The murine gene p27Kip1 is haplo-insufficient for tumour suppression. *Nature* **396:** 177–180.

Fogarty, P., S.D. Campbell, R. Abu-Shumays, B.S. Phalle, K.R. Yu, G.L. Uy, M.L. Goldberg, and W. Sullivan. 1997. The Drosophila grapes gene is related to checkpoint gene chk1/rad27 and is required for late syncytial division fidelity. *Curr. Biol.* **7:** 418–426.

Furnari, B., N. Rhind, and P. Russell. 1997. Cdc25 mitotic inducer targeted by chk1 DNA damage checkpoint kinase. *Science* **277:** 1495–1497.

Hakem, R., J.L. de la Pompa, C. Sirard, R. Mo, M. Woo, A. Hakem, A. Wakeham, J. Potter, A. Reitmair, F. Billia et al. 1996. The tumor suppressor gene Brca1 is required for embryonic cellular proliferation in the mouse. *Cell* **85:** 1009–1023.

Hirao A., Y. Kong, S. Matsuoka, A. Wakeham, J. Ruland, H. Yoshida, D. Liu, S.J. Elledge, and T.W. Mak. 2000. DNA damage-induced activation of p53 by the checkpoint kinase Chk2. *Science* **287:** 1824–1827.

Jones, J.M., X.-S. Cui, D. Medina, and L.A. Donehower. 1999. Heterozygosity of p21 WAF1/CIP1 enhances tumor cell proliferation and cyclin D1-associated kinase activity in a murine mammary cancer model. *Cell Growth Differ.* **10:** 213–222.

Kastan, M.B., Q. Zhan, W.S. el-Deiry, F. Carrier, T. Jacks, W.V. Walsh, B.S. Plunkett, B. Vogelstein, and A.J. Fornace. 1992. A mammalian cell cycle checkpoint pathway utilizing p53 and GADD45 is defective in ataxia-telangiectasia. *Cell* **71:** 587–597.

Keegan, K.S., D.A. Holtzman, A.W. Plug, E.R. Christenson, E.E. Brainerd, G. Flaggs, N.J. Bentley, E.M. Taylor, M.S. Meyn, S.B. Moss et al. 1996. The Atr and Atm protein kinases associate with different sites along meiotically pairing chromosomes. *Genes & Dev.* **10:** 2423–2437.

Kim, S.T., D.S. Lim, C.E. Canman, and M.B. Kastan. 1999. Substrate specificities and identification of putative substrates of ATM kinase family members. *J. Biol. Chem.* **274:** 37538–37543.

Kumagai, A. and W.G. Dunphy. 1999. Binding of 14-3-3 proteins and nuclear export control the intracellular localization of the mitotic inducer Cdc25. *Genes & Dev.* **13:** 1067–1072.

Kumagai A., Z. Guo, K.H. Emami, S.X. Wang, and W.G. Dunphy. 1998. The Xenopus Chk1 protein kinase mediates a caffeine-sensitive pathway of checkpoint control in cell-free extracts. *J. Cell. Biol.* **142:** 1559–1569.

Lim, D.S. and P. Hasty. 1996. A mutation in mouse rad51 results in an early embryonic lethal that is suppressed by a mutation in p53. *Mol. Cell. Biol.* **16:** 7133–7143.

Lindsay, H.D., D.J. Griffiths, R.J. Edwards, P.U. Christensen, J.M. Murray, F. Osman, N. Walworth, and A.M. Carr. 1998. S-phase-specific activation of Cds1 kinase defines a subpathway of the checkpoint response in *Schizosaccharomyces pombe*. *Genes & Dev.* **12:** 382–395.

Lopez-Girona, A., B. Furnari, O. Mondesert, and P. Russell. 1999. Nuclear localization of Cdc25 is regulated by DNA damage and a 14-3-3 protein. *Nature* **397:** 172–175.

Lu, X. and D.P. Lane. 1993. Differential induction of transcriptionally active p53 following UV or ionizing radiation: Defects in chromosome instability syndromes? *Cell* **75:** 765–778.

Luo, G., M.S. Yao, C.F. Bender, M. Mills, A.R. Bladl, A. Bradley, and J.H. Petrini. 1999. Disruption of mRad50 causes embryonic stem cell lethality, abnormal embryonic development, and sensitivity to ionizing radiation. *Proc. Natl. Acad. Sci.* **96:** 7376–7381.

Matsuoka, S., M. Huang, and S.J. Elledge. 1998. Linkage of ATM to cell cycle regulation by the Chk2 protein kinase. *Science* **282:** 1893–1897.

Nakajo, N., T. Oe, K. Uto, and N. Sagata. 1999. Involvement of Chk1 kinase in prophase I arrest of Xenopus oocytes. *Dev. Biol.* **207:** 432–444.

O'Connell, M.J., J.M. Raleigh, H.M. Verkade, and P. Nurse. 1997. Chk1 is a wee1 kinase in the G2 DNA damage checkpoint inhibiting cdc2 by Y15 phosphorylation. *EMBO J.* **16:** 545–554.

Parchment, R.E. 1991. Programmed cell death (apoptosis) in murine blastocysts: Extracellular free-radicals, polyamines, and other cytotoxic agents. *In Vivo* **5:** 493–500.

Peng, C-Y., P.R. Graves, R.S. Thoma, Z. Wu, A.S. Shaw, and H. Piwnica-Worms. 1997. Mitotic and G2 checkpoint control: Regulation of 14-3-3 protein binding by phosphorylation of Cdc25C on serine-216. *Science* **277:** 1501–1505.

Sanchez, Y., B.A. Desany, W.J. Jones, Q. Liu, B. Wang, and S.J. Elledge. 1996. Regulation of RAD53 by the ATM-like kinases MEC1 and TEL1 in yeast Cell Cycle Checkpoint Pathways. *Science* **271:** 357–360.

Sanchez, Y., C. Wong, R.S. Thoma, R. Richman, Z. Wu, H. Piwnica-Worms, and S.J. Elledge. 1997. Conservation of the Chk1 checkpoint pathway in mammals: Linkage DNA damage to Cdk regulation through Cdc25. *Science* **277:** 1497–1501.

Sanchez, Y., J. Bachant, H. Wang, F. Hu, D. Liu, M. Tetzlaff, and S.J. Elledge. 1999. Control of the DNA damage checkpoint by chk1 and rad53 protein kinases through distinct mechanisms. *Science* **286:** 1166–1171.

Savitsky, K., A. Bar-Shira, S. Gilad, G. Rotman, Y. Ziv, L. Vanagaite, D.A. Tagle, S. Smith, T. Uziel, S. Sfez et al. 1995. A single ataxia telangiectasia gene with a product similar to PI-3 kinase. *Science* **268:** 1749–1753.

Sharan, S.K., M. Morimatsu, U. Albrecht, D.S. Lim, E. Regel, C. Dinh, A. Sands, G. Eichele, P. Hasty, and A. Bradley. 1997. Embryonic lethality and radiation hypersensitivity mediated by Rad51 in mice lacking Brca2. *Nature* **386:** 804–810.

Shieh, S.Y., J. Ahn, K. Tamai, Y. Taya, and C. Prives. 2000. The human homologs of checkpoint kinases chk1 and cds1

(Chk2) phosphorylate p53 at multiple DNA damage-inducible sites. *Genes & Dev.* **14:** 289–300.

Sibon, O.C., V.A. Stevenson, and W.E. Theurkauf. 1997. DNA-replication checkpoint control at the Drosophila midblastula transition. *Nature* **388:** 93–97.

Sibon, O.C., A. Laurencon, R. Hawley, and W.E. Theurkauf. 1999. The Drosophila ATM homologue Mei-41 has an essential checkpoint function at the midblastula transition. *Curr. Biol.* **9:** 302–312.

Su, T.T., S.D. Campbell, and P.H. O'Farrell. 1999. Drosophila grapes/CHK1 mutants are defective in cyclin proteolysis and coordination of mitotic events. *Curr. Biol.* **9:** 919–922.

Sun, Z., D.S. Fay, F. Marini, M. Foiani, and D.F. Stern. 1996. Spk1/Rad53 is regulated by Mec1-dependent protein phosphorylation in DNA replication and damage checkpoint pathways. *Genes & Dev.* **10:** 395–406.

Tibbetts, R.S., K.M. Brumbaugh, J.M. Williams, J.N. Sarkaria, W.A. Cliby, S.Y. Shieh, Y. Taya, C. Prives, and R.T. Abraham. 1999. A role for ATR in the DNA damage-induced phosphorylation of p53. *Genes & Dev.* **13:** 152–157.

Tsukamoto, A.S., R. Grosschedl, R.C. Guman, T. Parslow, and H.E. Varmus. 1988. Expression of the *int-1* gene in transgenic mice is associated with mammary gland hyperplasia and adenocarcinomas in male and female mice. *Cell* **55:** 619–625.

Venkatachalam, S., Y.P. Shi, S.N. Jones, H. Vogel, A. Bradley, D. Pinkel, and L.A. Donehower. 1998. Retention of wild-type p53 in tumors from p53 heterozygous mice: Reduction of p53 dosage can promote cancer formation. *EMBO J.* **17:** 4657–4667.

Walworth, N.C. and R. Bernards. 1996. Rad-dependent response of the chk1-encoded protein kinase at the DNA damage checkpoint. *Science* **271:** 353–356.

Walworth, N., S. Davey, and D. Beach. 1993. Fission yeast chk1 protein kinase links the rad checkpoint pathway to cdc2. *Nature* **363:** 368–371.

Wright, J.A., K.S. Keegan, D.R. Herendeen, N.J. Bentley, A.M. Carr, M.F. Hoekstra, and P. Concannon. 1998. Protein kinase mutants of human ATR increase sensitivity to UV and ionizing radiation and abrogate cell cycle checkpoint control. *Proc. Natl. Acad. Sci.* **95:** 7445–7450.

Xu, Y., T. Ashley, E.E. Brainerd, R.T. Bronson, M.S. Meyn, and D. Baltimore. 1996. Targeted disruption of ATM leads to growth retardation, chromosomal fragmentation during meiosis, immune defects, and thymic lymphoma. *Genes & Dev.* **10:** 2411–2422.

Yamaguchi-Iwai, Y., E. Sonoda, M.S. Sasaki, C. Morrison, T. Haraguchi, Y. Hiraoka, Y.M. Yamashita, T. Yagi, M. Takata, C. Price et al. 1999. Mre11 is essential for the maintenance of chromosomal DNA in vertebrate cells. *EMBO J.* **18:** 6619–6629.

Yang, J., K. Winkler, M. Yoshida, and S. Kornbluth. 1999. Maintenance of G2 arrest in the Xenopus oocyte: A role for 14-3-3-mediated inhibition of Cdc25 nuclear import. *EMBO J.* **18:** 2174–2183.

Differential Gene Expression in Mouse Mammary Adenocarcinomas in the Presence and Absence of Wild Type p53

Xian-Shu Cui[1] and Lawrence A. Donehower[1,2*]

[1]Department of Molecular Virology and Microbiology and [2]Department of Molecular and Cellular Biology, Baylor College of Medicine, Houston, TX 77030

*Correspondence to: Lawrence A. Donehower
Department of Molecular Virology and Microbiology
Baylor College of Medicine
One Baylor Plaza
Houston, TX 77030

Keywords: p53, mouse mammary tumor, *Wnt-1*, $p21^{WAF1/CIP1}$, c-*kit*, cyclin B1

Running Title: p53 effects on gene expression in mammary tumors

Abstract

The tumor suppressor p53 transcriptionally regulates a large number of target genes that may affect cell growth and cell death pathways. To better understand the role of p53 loss in tumorigenesis, we have developed a mouse mammary cancer model, the *Wnt-1* TG/p53 model. *Wnt-1* transgenic females that are p53-/- develop mammary adenocarcinomas that arise sooner, grow faster, appear more anaplastic, and have higher levels of chromosomal instability than their *Wnt-1* transgenic p53+/+ counterparts. In this study, we used several assays to determine whether the presence or absence of p53 affects gene expression patterns in the mammary adenocarcinomas. Most of the differentially expressed genes are increased in p53+/+ tumors and many of these represent known target genes of p53 ($p21^{WAF1/CIP1}$, cyclin G1, alpha smooth muscle actin, and cytokeratin 19). Some of these genes (cytokeratin 19, alpha smooth muscle actin, and kappa casein) represent mammary gland differentiation markers which may contribute to the inhibited tumor progression and are consistent with the more differentiated histopathology observed in the p53+/+ tumors. Several differentially expressed genes are growth regulatory in function (p21, c-*kit*, and cyclin B1) and their altered expression levels correlate well with the differing growth properties of the p53+/+ and p53-/- tumors. Thus, while tumors can arise and progress in the presence of functioning wild type p53, p53 may directly or indirectly regulate expression of an array of genes that facilitate differentiation and repress proliferation, contributing to a more differentiated, slow growing, and genomically stable phenotype.

Introduction

The p53 tumor suppressor gene is lost or mutated in over half of all human cancers (Levine, 1997; Lozano and Elledge, 2000). In addition, inactivation of p53 function without loss of p53 structural integrity may occur by a number of different mechanisms (Moll *et al.*, 1998; Freedman *et al.*, 1999). Nevertheless, a significant fraction of human tumors arise and progress without incurring mutation or functional loss of p53 activity. In such tumors, retention of p53 activity has important clinical consequences. These tumors often have better prognoses and better responses to chemotherapeutic regimens (Kirsch and Kastan, 1998; Wallace-Brodeur and Lowe, 1999). Moreover, some tumor types with intact p53 exhibit less anaplastic histopathology, lower proliferation levels, and less chromosomal instability (Donehower, 1996).

The p53 protein is a transcriptional regulatory factor that responds to a number of cellular stresses, including DNA damage and activated cellular oncogenes (Giaccia and Kastan, 1998). The activated p53 protein can transactivate a number of genes involved either in cell cycle control or in cell apoptosis pathways (el-Deiry, 1998). One of the first identified targets of p53 was the $p21^{WAF1/CIP1}$ cyclin-dependent kinase inhibitor, which directly interacts with G1 cyclin-cdk complexes and inhibits their activity, and thus is an important component of the p53-mediated G1 arrest checkpoint (el Deiry et al., 1993; Harper et al., 1993). Another important p53 target relevant to the apoptotic function of p53 is bax, a pro-apoptotic protein (Mayashita and Reed, 1995). Recently, the introduction of large scale screening technologies has greatly increased the number of known p53 targets. Using techniques such as serial analysis of gene expression (SAGE) and cDNA array analyses, a library of genes have been assembled that are either upregulated or downregulated by p53 (Polyak *et al.*, 1999; Yu *et al.*, 1999; Zhao *et al.*, 2000). Some of these genes regulate cell growth or death control, but others appear to be

involved in physiological processes not directly related to growth or death (Polyak et al., 1997; Zhao et al., 2000). Moreover, there is a great deal of heterogeneity in the response of p53 target genes. A number of factors influence the types of p53-responsive genes that are activated or repressed, including p53 levels, the nature of the cellular stress, and the cell type being studied (Yu *et al.*, 1999; Zhao *et al.*, 2000).

While the SAGE and cDNA array screens have provided powerful tools for the identification of novel p53 target genes, there are potential limitations in the use of such screens. Generally, very high levels of p53 are often produced, which may fail to identify target genes regulated by physiological levels of p53. In addition, cancer cell lines of various types are often used and these cells have other genetic defects which may prevent identification of bona fide p53 targets. Finally, the experiments are performed in cell culture, and so targets may be missed that result from the activation of p53 in its normal in vivo context.

To circumvent some of these potential limitations and identify genes regulated by p53 in vivo which might be directly relevant to tumorigenesis, we have utilized a murine mammary cancer model, the *Wnt-1* TG/p53 mouse. *Wnt-1* TG mice contain several copies of a germline *Wnt-1* oncogene driven by a mammary gland specific mouse mammary tumor virus promoter (Tsukamoto *et al.*, 1988). The female *Wnt-1* transgenic mice develop early mammary gland hyperplasia and usually succumb to mammary adenocarcinomas between the ages of 3 and 12 months. In order to determine the effects of p53 dosage on mammary tumorigenesis in this model, we crossed the *Wnt-1* TG mice to p53-deficient mice and the *Wnt-1* transgenic female offspring were monitored for mammary tumors in the presence and absence of p53 (Donehower et al., 1995). As shown in Table 1, the absence of p53 (p53-/-) in the presence of the *Wnt-1* transgene resulted in mammary tumors that appeared sooner, grew faster, displayed less

differentiated and more anaplastic histopathology, and exhibited much more chromosomal instability than their *Wnt-1* TG p53+/+ counterparts (Donehower et al., 1995; Jones et al., 1997). Moreover, these differences in tumorigenic phenotypes were likely to be due directly to p53 status, since the p53 gene was not mutated or suppressed in the p53+/+ tumors (Donehower et al., 1995).

Because the p53+/+ and p53-/- *Wnt-1* TG mice generate the same type of mammary adenocarcinomas, we decided to compare their gene expression patterns, on the hypothesis that differences in gene expression might be relevant to p53 status and the observed tumorigenic phenotypes. While we believe there are a number of advantages of our in vivo tumorigenesis model (e.g. a closer approximation to real physiological conditions), there may also be at least three potential limitations not encountered in the in vitro screens. First, mammary tumors are heterogeneous and not composed solely of tumor cells. They are a mixture of epithelial tumor cells, myoepithelial and stromal components, adipose cells, and blood vessels. However, we have found that the epithelial tumor component usually predominates and thus the other nontumor components should not obscure any strong differences in gene expression. Second, despite being of identical histopathological type, intertumoral variation may be significant and apparent differences might be due to such variation rather than p53 status. To address this problem we analyzed expression patterns in five to eight different tumors of each p53 genotype. Thus, if all or almost all p53+/+ tumors show higher expression levels of a particular gene than is seen in their p53-/- counterparts, then this difference is likely to be significant. Finally, comparison of end stage p53+/+ and p53-/- tumors will not necessarily identify direct p53 targets. Instead, secondary p53 targets or genes altered in expression due to other genetic changes might be detected. While this is a valid concern, our discovery that many of the differentially regulated genes in our tumor model

are known p53 target genes has reassured us that, in many cases, the differential expression is likely to be due directly to p53 expression levels.

Using several different approaches, we show here that, in addition to altering biological and genetic properties of mammary adenocarcinomas, p53 status affects gene expression patterns. At least eight differentially expressed genes have been identified in comparing p53+/+ and p53-/- tumors. Some of the differentially expressed genes are clearly related to growth control, while others appear to be differentiation markers. The observed differential expression patterns of particular genes fit well with the biological properties of the parental tumors, suggesting that these genes may be a cause rather than an effect of the tumor phenotype. Thus, these results may provide further insights into the role of p53 target genes in the pleiotropic biological effects associated with tumorigenesis.

Results

Differentially expressed genes identified by differential display PCR

To identify differentially expressed genes in *Wnt-1* TG p53+/+ and *Wnt-1* TG p53-/- tumors, we utilized several different types of screening methods. RNA differential display and cDNA array methods were used to randomly screen the tumors for differentially expressed genes. In addition, Northern blot and RNAse protection assays were employed to investigate specific known candidate genes. Each of these approaches revealed differentially expressed genes. Our first set of experiments employed RNA differential display PCR to screen tumor RNAs from *Wnt-1* TG p53+/+, *Wnt-1* TG p53+/- LOH, and *Wnt-1* TG p53-/- tumors (Liang and Pardee, 1992). The *Wnt-1* TG p53+/- LOH tumors are null for p53 because the remaining p53 wild type allele has been deleted during mammary tumorigenesis (Donehower *et al.*, 1995). A number of candidate fragments were identified by this PCR-based method. An example of a fragment specific for the p53+/+ tumor RNAs is shown in Fig. 1A. All fragments identified in this assay were at increased levels in the p53+/+ tumors. These p53+/+ specific fragments were then excised from the gel, reamplified with the appropriate differential display primers, labeled with ^{32}P and used as probes on Northern blots containing total RNAs from five p53+/+ and five p53-/- tumors. Three separate differential display fragments consistently showed higher hybridization levels in the five p53+/+ tumors. These fragments were cloned and sequenced. The sequences were then compared with the GenBank database and were shown to be identical to three murine genes: alpha smooth muscle actin, kappa casein, and aldolase C. The murine cDNA sequences of each of these three genes were then obtained and used to probe a Northern blot containing total RNAs from eight p53+/+ mammary adenocarcinomas and eight p53-/- adenocarcinomas (Fig. 1B). Note that while there is heterogeneity in the RNA levels

of each gene from tumor to tumor, when the hybridization levels are quantitated and normalized to control probe (GAPDH) hybridization intensity, significant increases in RNA levels of these three genes are observed in p53+/+ tumors. Alpha smooth muscle actin RNA levels were on average 4.2 fold higher in p53+/+ tumors compared to p53-/- tumors. Kappa casein and aldolase C had a mean increase of 3.2 and 2.9, respectively, compared to p53-/- tumors. These differences were significant at the 0.05 level as measured by t test.

Differentially expressed genes identified by cDNA array analysis

As an adjunct to the differential display analyses, we probed array filters containing 588 murine cDNAs (from Clontech) with ^{32}P-labeled cDNA probes prepared from mRNA derived from either p53+/+ or p53-/- tumors. There were two genes that consistently showed differential expression by this method: c-*kit* and cytokeratin 19 (Fig. 2A). Both genes showed higher levels of hybridization in the p53+/+ tumors. cDNAs from cytokeratin 19 and c-*kit* were labeled with ^{32}P and hybridized to Northern blots containing mRNAs from multiple p53+/+ and p53-/- tumors. Again, while there was considerable heterogeneity in expression levels, the c-*kit* and cytokeratin 19 genes averaged 2.4 and 2.7 fold increases in expression in p53+/+ tumors compared to p53-/- tumors (Fig. 2B,C). These differences were found to be significant by t test.

Examination of known p53 target genes

Those p53 target genes known to regulate growth control were obvious candidates for analysis. The prototype p53 target gene is p21$^{WAF1/CIP1}$, a cyclin-dependent kinase inhibitor (el-Deiry *et al.*, 1993; Harper *et al.*, 1993). Northern blot analysis of p53+/+ and p53-/- tumor RNAs using a murine p21$^{WAF1/CIP1}$ cDNA probe revealed that the p53+/+

tumors averaged 2.3 fold higher levels of p21 compared to the p53-/- tumors (Fig. 3), consistent with the reduced growth rates observed in the p53+/+ tumors. These differences were shown to be statistically significant.

Other important cell cycle regulatory proteins are the cyclins. At least two of these, cyclin B1 and cyclin G1, have been shown to be regulated by p53 (Innocente *et al.*, 1999; Taylor *et al.*, 1999; Okamoto and Beach, 1994). Cyclin B1 appears to be directly repressed by p53 and cyclin G1 has been shown to be upregulated by wild type p53. The cyclin mRNA levels were assessed in p53+/+ and p53-/- tumors by RNAse protection assay using kits specific for murine cyclin mRNAs. Interestingly, the only cyclins to show significant differential expression after normalization to the GAPDH control RNA were cyclin B1 (Fig. 4A) and cyclin G1 (Fig. 4B). p53-/- tumors averaged 2.3 fold higher cyclin B1 than p53+/+ tumors and p53+/+ tumors showed 1.8 fold elevated levels of cyclin G1 compared to p53-/- tumors. Again, these differences were found to be significant by t test.

Differential protein expression levels

To correlate protein expression levels with the differentially expressed RNAs in the tumors, we performed Western blot analyses on extracts from p53+/+ and p53-/- tumors. Figure 5A shows that all of the p53+/+ tumors show high levels of alpha smooth muscle actin while only one of the six p53-/- tumors shows comparably high protein levels. Likewise, c-kit protein levels were generally higher in the p53+/+ tumors than their p53-/- counterparts, consistent with the earlier RNA results (Fig. 5B). p53+/+ tumors also showed higher levels of cytokeratin 19 than p53-/- tumors (Fig. 5B). Finally, cyclin B1 protein levels were higher in the majority of p53-/- tumors than in p53+/+ tumors (Fig. 5C), again correlating well with the RNA data for this gene.

Discussion

We believe that the *Wnt-1* TG/p53 model provides a number of advantages for mechanistic studies on the role of p53 in tumorigenesis. Virtually all of the *Wnt-1* TG females develop only mammary adenocarcinomas within 2-9 months either in the presence or absence of p53. In our model, the absence of p53 has been shown to dramatically alter the biological and genetic properties of the *Wnt-1*-initiated adenocarcinomas. An important question is whether the more aggressive and malignant characteristics of the p53-/- tumors are a direct result of the absence of p53 or an indirect result of the genomic instability promoted by the lack of p53. In this latter scenario, the driving force for tumor initiation and progression would be the increased rate of cooperating genetic lesions in the p53-/- tumors. However, if p53 were playing a more active role in inhibition of tumor growth through its transcriptional regulatory function, then upregulation of p53 growth inhibitory targets and downregulation of p53 growth stimulatory targets might be observed. In fact, the increase in p21 and cyclin G1 levels and decreased cyclin B1 levels observed in the p53+/+ tumors are consistent with a direct role for p53 in modulating tumor growth rates. Moreover, the upregulation of several differentiation markers in the p53+/+ tumors, some direct targets of p53, suggests that these genes may be contributing to some of the biological properties of the tumors. Finally, the increased activities of the known p53 target genes in the p53+/+ tumors indicates that p53 signaling pathways are intact in these tumors, and that tumors can readily arise in this model in the presence of functional p53.

The differentially expressed genes that have been identified in this model fall generally into two categories, growth regulatory genes (p21, cyclin G1, cyclin B1, and c-*kit*) and differentiation markers (alpha smooth muscle actin, kappa casein, aldolase C, and cytokeratin 19). Some of the other categories of p53 target genes found in cell based

screens, such as apoptosis-related genes and genes which regulate reactive oxygen species formation, have not been identified as differentially expressed genes in any of our tumor screens. This finding agrees with earlier findings by Yu et al. (1999) that the responses by p53 targets can vary considerably from cell line to cell line. Moreover, because in our model p53 is expressed at physiological levels in an in vivo heterogeneous context of mixed cell types, it is not surprising that the range of p53 targets observed is quite different from the cell based screens. However, the specific nature of the genes that are differentially expressed in our model is consistent with their playing a direct role in modulating the biological properties of the tumors. The potential relevance of each differentially expressed gene to the tumorigenesis process is discussed below.

Differentially expressed growth regulatory genes

$p21^{WAF1/CIP1}$. $p21^{WAF1/CIP1}$ is a protypical p53 target gene activated by p53 in response to a variety of cell stresses (Gorospe et al., 1999). It is a cyclin-dependent kinase inhibitor which has both G1 and G2 checkpoint functions in response to DNA damage (Harper et al., 1995; Dulic et al, 1998; Bunz et al., 1998). Its higher levels of expression in the presence of p53 may directly reduce tumor growth rates as observed in previous studies on the *Wnt-1* TG model. In these studies we found that *Wnt-1* TG p21+/- mammary tumors had dramatically higher growth rates compared to *Wnt-1* TG p21+/+ tumors (Jones et al., 1999). In addition, maintenance of G1 and G2 checkpoints in the p53+/+ tumors (in part through increased p21) may also contribute to the relatively high levels of genomic stability observed in this category of tumors.

Cyclin B1. Cyclin B1 is the major cyclin component of the mitotic cdc2-cyclin B complex initiatiating mitosis in eukaryotic cells (Musunuru and Hinds, 1997). It is upregulated in expression in the G2/M phase of the cell cycle. Recently, it has been

demonstrated that p53 directly represses transcription of the cyclin B1 gene and thus may affect G2/M transition by reducing intracellular cyclin B1 levels (Innocente *et al.*, 1999; Taylor *et al.*, 1999). p21 has also been shown to inhibit the kinase activity of the cyclin B1-cdc2 complex (Xiong et al., 1993; Harper et al., 1995) and so p53 may mediate the G2 checkpoint through multiple mechanisms. Such mechanisms may contribute to the reduced rate of cell cycle progression and genomic stability observed in the p53+/+ tumors (Donehower et al., 1995; Jones *et al.*, 1997).

Cyclin G1. Cyclin G1 has been shown to be transcriptionally activated by p53 in response to DNA damage (Okamoto and Beach, 1994). The role of cyclin G1 in cell cycle control has not been established and published reports are contradictory as to whether cyclin G1 is growth promoting or growth inhibitory (Smith et al., 1997; Shimizu et al., 1998). Recently, however, it has been shown that overexpression of cyclin G augments the apoptosis process (Okamoto and Prives, 1999). However, since apoptosis levels are low in the p53+/+ tumors, it is not clear how increased cyclin G1 levels in these tumors might affect their biological properties.

c-kit. c-*kit* encodes a membrane tyrosine kinase receptor and is not known to be a direct target of p53. Its ligand is stem cell factor, which promotes growth in a number of hematopoietic precursor types (Ashman, 1999). Mutated versions of kit can be oncogenic and it is expressed at high levels in small cell lung carcinomas (Hibi et al., 1991). However, in other types of human cancers, such as melanomas, thyroid carcinomas, and breast cancers, c-*kit* expression was reduced as the tumors progressed from normal tissues to benign lesions to malignant cancers (Natali et al., 1992a; Natali et al., 1992b; Natali et al., 1995). Moreover, ectopic expression of c-*kit* in breast cancer

cells suppressed their growth (Nishida et al., 1996), indicating that in mammary cells, c-*kit* may act as a tumor suppressor. Thus, in our mammary cancer model, the increased expression of c-*kit* in the p53+/+ tumors may not only be a marker for a less malignant status, but may also be directly active in suppressing tumor cell growth rates.

Differentially expressed differentiation markers

Alpha smooth muscle actin. Alpha smooth muscle actin is a major component of microfilaments and assists in maintaining cell shape and movement. It has been shown to be a p53 target gene (Comer et al., 1998) and is also a marker for the myoepithelial cell compartment of the mammary gland (Gugliotta et al., 1988). Interestingly, alpha smooth muscle actin is downregulated in transformed cells and an inverse relationship between cellular proliferation and alpha smooth muscle actin expression has been widely observed (Leavitt et al., 1985; Owens et al., 1986). In the p53+/+ tumors, it appears to be highly expressed in myoepithelial cells, a compartment which is virtually non-existent in the p53-/- tumors (X.C. and L.D., unpublished data). Thus, higher expression levels of this p53 responsive gene is a good indicator of retention of more differentiated cell types in the p53+/+ tumors. Whether alpha smooth muscle actin has any role in the inhibition of tumor growth rates remains unclear.

Cytokeratin 19. Cytokeratin 19 is one of the constituents of the intermediate filaments of epithelial cells and has recently been shown to be a p53 target gene (Moll, 1998; Zhao et al., 2000). Cytokeratin 19 is a widely used luminal cell epithelial marker which is expressed at high levels in both normal and malignant human mammary epithelial cells (Moll, 1998). It is expressed at high levels in many of the p53+/+ tumors, indicating the presence of significant numbers of luminal epithelial cells in the tumors. However, the

p53-/- tumors display lower levels of cytokeratin 19 mRNA and protein, indicating that either these tumors have lost most of their luminal epithelial cells or that the luminal epithelial cells in these tumors have somehow lost cytokeratin 19 expression.

Kappa casein. Kappa casein is not considered to be a p53 target, but is a milk protein specific for secretory alveolar cells in the mammary gland (Ginger and Grigor, 1999). It is found at high levels in normal breast tissue, lower levels in benign lesions, and not at all in invasive carcinomas (Rudland et al., 1993). Its increased levels in the p53+/+ tumors are consistent with the relatively differentiated state of these tumors. It also indicates retention of some functional secretory alveolar cells in the p53+/+ tumors and their loss in the more dedifferentiated p53-/- tumors.

Aldolase C. Aldolase C is not known to be a p53 target and is not a specific epithelial cell marker, but rather a CNS-specific glycolytic enzyme (Seidenfeld and Marton, 1979). Why it was identified in our screen is not clear, but it is often expressed at higher levels in the p53+/+ tumors.

Conclusions

The identification of differentially expressed growth-related genes in our model is consistent with the observed differences in tumor growth rates between the p53+/+ and p53-/- mice. Interestingly, three of four of these genes are p53 target genes, indicating that wild type p53 is actively regulating expression of these genes. We hypothesize that such p53 signaling inhibits cell cycle progression in the p53+/+ tumor cells and may be at least partially responsible for their slower growth rate. The retention of G1 and G2 checkpoint control in the p53+/+ tumors may also contribute to the slower growth rate

and delayed tumor incidence by preventing genomic instability and the resultant increase in oncogenic mutations.

The higher expression of differentiation markers in the p53+/+ tumors, such as alpha smooth muscle actin and kappa casein, is consistent with their more differentiated histopathological appearance. Since these two genes have been associated with myoepithelial and secretory alveolar cell types, respectively, it is likely that such differentiated cell types are lost in the progression of the p53-/- tumors to a more dedifferentiated state. In human breast neoplasms, benign lesions show retention of myoepithelial and secrectory alveolar cells, while in invasive carcinomas they are almost completely lost (Rudland et al., 1993). Thus, our p53+/+ tumors are likely to represent a more benign stage of mammary tumor progression, while the p53-/- tumors may be models for the more invasive stages of mammary carcinomas.

Despite the limitations inherent in doing expression analyses on end stage heterogeneous tumors, differentially expressed genes were identified in multiple p53+/+ and p53-/- tumors. The differentially expressed genes that were obtained were either growth regulators or indicators of cell differentiation status and were consistent with the differential histopathology and biological properties of the p53+/+ and p53-/- tumors. Moreover, these results and the fact that many of these genes were bona fide direct transcriptional targets of p53 lends support to our argument that screening of whole tumors is a viable approach for identifying such genes. Further screens with large cDNA arrays should reveal additional differentially expressed genes. A remaining challenge will be to determine which of these differentially expressed genes have a direct effect on the biological properties of the mammary adenocarcinomas.

Materials and Methods

Tumor samples

The *Wnt-1* TG/p53 mammary cancer model from which the mammary tumors have been obtained has been previously described (Donehower *et al.*, 1995). *Wnt-1* TG p53+/+, *Wnt-1* TG p53+/-, and *Wnt-1* TG p53-/- females were monitored for tumors on a weekly basis from the time of weaning until the first observation of tumors. Four weeks after first observation of a tumor, the tumor bearing animal was sacrificed and the tumor excised. The skin and connective tissue were removed carefully and part of the tumor was placed in 10% neutral buffered formalin and the remainder was frozen in an Eppendorf tube at –80° C. The tumor segment in formalin was then fixed in paraffin and hematoxylin and eosin stained slides made from 4 μ sections of tumor tissue. These sections were then typed by histopathological examination and virtually all were categorized as Dunn type B mammary adenocarcinomas. In preparation for the various RNA assays described below, mRNA was purified from frozen tumor segments utilizing the Invitrogen mRNA extraction kit according to the manufacturer's specifications.

Differential display

The Clontech Delta Differential Display kit was used to screen tumor RNAs derived from p53+/+ and p53-/- mammary tumors. RNAs from p53+/- tumors that had lost their remaining wild type p53 allele (p53+/- LOH) were also utilized. These tumors were similar in their histopathological and biologic properties to p53-/- tumors. The protocols were all performed according to the manufacturer's instructions and will only be outlined here. Initially, the first strand cDNA is synthesized from each of the tumor RNA populations of interest, using murine leukemia virus reverse transcriptase and oligo(dT) as a primer. For differential display PCR, ten arbitrary 5' primers (oligo(dT)$_9$-

NN, where N = A,G, or C) were combined with ten arbitrary 3' primers randomly in a PCR reaction in the presence of alpha-^{33}P-dATP. To resolve the PCR-amplified labeled cDNA fragments, a denaturing 5% polyacrylamide/8 M urea gel was used. After electrophoresis, the denaturing gels were subjected to autoradiography and the X-ray films were carefully examined for differentially expressed bands. Generally, multiple tumor RNAs of each genotype were run in parallel to identify fragments which were consistently overexpressed or underexpressed in a particular genotype. Once differentially expressed bands were identified, they were excised from the gel, placed in TE buffer (10 mM Tris-HCl, pH 8.0, 1 mM EDTA), and the cDNA fragments were eluted from the gel slice by boiling. The DNA was then reamplified using the original 5' and 3' arbitrary primers. ^{32}P-labeled probes were made from the reamplified fragments by the random primed oligo labeling procedure using the Roche High Prime kit and used to probe Northern blots of RNAs from 6-8 p53+/+ and 6-8 p53-/- tumors. Those probes that showed consistent p53 genotype-specific overexpression or underexpression were ligated into a Clontech TA cloning vector using the Clontech AdvanTAge PCR cloning kit according to the manufacturer's specifications. Positive clones were amplified and sequenced with the M13 forward primer and the Amersham Sequenase kit. About 200-300 base pairs of insert sequences were identified by this method and these were used to probe GenBank in homology searches.

Northern blot hybridization

For Northern blot analysis, the Ambion NorthernMax kit was used according to manufacturer directions. Two μg of mRNA from 5-8 p53+/+ tumors and 5-8 p53-/- tumors were loaded in each well of the agarose gel. After electrophoresis, the separated RNAs were transferred to a Zeta-Probe membrane from Bio-Rad. Labelled ^{32}P probes for

each differentially expressed gene were hybridized to the membranes. After hybridization, membrane washing, and autoradiography, the band hybridization intensities on the filters were quantitated on the Molecular Dynamics Storm 860 Phosphorimager. The filters were then stripped and reprobed with a labeled GAPDH probe to provide a normalization control. After autoradiography, this filter was also subjected to phosphorimager analysis. Relative hybridization intensities for a particular gene in a tumor were always normalized to the intensity of the GAPDH signal in that tumor to obtain quantitative values.

cDNA arrays

The Clontech Atlas mouse array I with 588 known cDNAs attached to duplicate nylon membranes was used for the cDNA array screen. One μg of mRNA from a p53-/- tumor and a p53+/+ tumor were each reverse transcribed in the presence of alpha ^{32}P-dATP. The labeled cDNA populations were then each hybridized overnight to the two array filters according to the manufacturer's specifications. After washing and autoradiography, the hybridization intensity of each of the genes on the filter was quantitated by phosphorimager analysis. Spot intensities were then normalized to the intensities of housekeeping genes on the filter to estimate relative hybridization levels between the p53+/+ and p53-/- filters. Genes that repeatedly showed more than 2.5 fold differences in hybridization intensity between the two filters were assessed for differential expression by Northern blot hybridization after synthesis of probes by RT-PCR using gene specific primers.

RNAse protection assay

RNA expression levels of 14 cyclin genes in the p53+/+ and p53-/- tumors were assessed using two Pharmingen multi-probe RNAse protection assay kits (mcyc-1 and mcyc-2). ^{32}P-labeled RNA mouse cyclin probes were generated by T7 RNA polymerase-directed synthesis of fourteen different cyclin gene templates. The multi-probe set was then hybridized in excess to target RNA (10 μg mRNA for each sample) in solution, after which free probes and other single-stranded RNA are digested with RNAses. The remaining RNAse protected probes were purified, resolved on denaturing polyacrylamide gels, and quantified by phosphorimaging. The quantity of each mRNA species in the original RNA sample could then be determined based on the intensity of the appropriately sized protected probe fragment following normalization to a control probe (GAPDH) used along with the cyclin probes.

Immunoblot assays

Western blot analysis of alpha smooth muscle actin, cytokeratin 19, c-*kit*, and cyclin B1 protein was performed from tumor lysates of multiple p53+/+ and p53-/- tumors. For alpha smooth muscle actin protein detection, 20 μg of total tumor lysate was run on an 8% SDS polyacrylamide gel. The gel was transferred to a 0.45 μm pore size nitrocellulose membrane (BA85, Schleicher & Schuell) for 2 hours at 75 volts and then blocked with 5% nonfat dry milk in Tris-buffered saline with 2% Tween 20 (TBST) overnight at 4° C. The blot was incubated with mouse monoclonal antibody for alpha smooth muscle actin (Clone 1A4 from NeoMarkers) diluted at 1:1000 in TBST with 1% nonfat dry milk for one hour at room temperature. After washing three times with TBST, the blot was incubated with goat anti-mouse IgG2a peroxidase. Protein was detected using the supersignal enhanced chemiluminescence (ECL) system (Pierce). For cytokeratin 19 detection, 50 μg protein lysate was loaded for gel separation. The

antibody used for cytokeratin 19 was Clone A53-B from NeoMarkers. Dilution and incubation conditions were the same as for alpha-smooth muscle actin. c-kit antibody (M-14, Santa Cruz) was diluted 1:200. Antigoat IgG was diluted 1:2000 as secondary antibody. For cyclin B1 detection, 20 μg protein lysate was loaded on an SDS-polyacrylamide gel. After transfer to a nitrocellulose membrane, the blot was incubated with a polyclonal antibody to cyclin B1 (Oncogene Research Ab-3) diluted 1:2000. Goat anti-rabbit antibody (SC-2030, Santa Cruz) was diluted 1:1000 as secondary antibody. Each blot was stripped and reprobed with an antibody against all six isoforms of vertebrate actin (C4, Boehringer-Mannheim) as a loading control.

Acknowledgments

We would like to thank Harold Varmus for providing us with the *Wnt-1* TG mice. We also thank Dan Medina for helpful discussions and for histopathological analyses of the tumors. This work was supported by grants from the National Cancer Institute and the U.S. Army Breast Cancer Program to L.D. L.D. is the recipient of an Academic Award from the U.S. Army Breast Cancer Program. X.C. was supported by the Karolinska Institute/Baylor College of Medicine Exchange Program and the U.S. Army Breast Cancer Research Program.

References

Ashman LK. (1999). *Int. J. Biochem. Cell Biol.* **31**, 1037-1051.

Bunz F, Dutriaux A, Lengauer C, Waldman T, Zhou S, Brown JP, Sedivy JM, Kinzler KW and Vogelstein B. (1998). *Science*, **282**, 1497-1501.

Comer KA, Dennis PA, Armstrong L, Catino JJ, Kastan MB and Kumar CC. (1998). *Oncogene*, **16**,1299-1308.

Donehower, LA. (1996). *Biochim. Biophys. Acta*, **1242**, 171-176.

Donehower LA, Godley LA, Aldaz CM, Pyle R, Shi YP, Pinkel D, Gray J, Bradley A, Medina D and Varmus HE. (1995). *Genes Dev.*, **9**, 882-895.

Dulic V, Stein GH, Far DF and Reed SI. (1998). *Mol Cell Biol.*, **18**, 1546-1557.

el-Deiry WS. (1998). *Semin. Cancer Biol.*, **8**, 345-357.

el-Deiry WS, Tokino T, Velculescu VE, Levy DB, Parsons R, Trent JM, Lin D, Mercer WE, Freedman DA, Wu L, Levine AJ. (1999). *Cell Mol Life Sci.*, **55**, 96-107.

Giaccia AJ and Kastan MB. (1998). *Genes Dev.*, **12**, 2973-2983.

Ginger MR and Grigor MR. (1999). Comp. *Biochem. Physiol. B Biochem. Mol. Biol.* **124**, 133-145.

Gorospe M, Wang X and Holbrook NJ. (1999). *Gene Expr.*, **7**,377-85.

Gugliotta P, Sapino A, Macri L, Skalli O, Gabbiani G and Bussolati G. (1988). *J. Histochem. Cytochem.*, **36**, 659-663.

Harper JW, Adami GR, Wei N, Keyomarsi K, Elledge SJ. (1993). *Cell*, **75**, 805-816.

Harper JW, Elledge SJ, Keyomarsi K, Dynlacht B, Tsai LH, Zhang P, Dobrowolski S, Bai C, Connell-Crowley L, Swindell E, et al. (1995). *Mol Biol Cell.*, **6**, 387-400.

Hibi K, Takahashi T, Sekido Y, Ueda R, Hida T, Ariyoshi Y, Takagi H and Takahashi T. (1991). *Oncogene,* **6**, 2291-2296.

Innocente SA, Abrahamson JL, Cogswell JP and Lee JM. (1999). *Proc Natl Acad Sci USA*, **96**, 2147-2152.

Jones JM, Attardi L, Godley LA, Laucirica R, Medina D, Jacks T, Varmus HE and Donehower LA. (1997). *Cell Growth Differ.*, **8**, 829-838.

Jones JM, Cui XS, Medina D and Donehower LA. (1999). *Cell Growth Differ.*, **10**, 213-222.

Kinzler KW, Vogelstein B. (1993). *Cell*, **75**, 817-825.

Kirsch DG, Kastan MB. (1998). *J. Clin. Oncol.*, **16**, 3158-3168.

Leavitt J, Gunning P, Kedes L and Jariwalla R. (1985). *Nature*, **316**, 840-842.

Levine AJ. (1997). *Cell*, **88**, 323-331.

Liang P and Pardee AB. (1992). *Science*, **257**, 967-971.

Lozano G and Elledge SJ. (2000). *Nature*, **404**, 24-25.

Miyashita T and Reed JC. (1995). *Cell*, **80**, 293-299.

Moll UM, Schramm LM. (1998). *Crit Rev Oral Biol Med.*, **9**, 23-37.

Musunuru K and Hinds PW. (1997). *Cell Cycle Regulators in Cancer*. Karger Landes Systems, Basel.

Natali PG, Nicotra MR, Winkler AB, Cavaliere R, Bigotti A and Ullrich A. (1992a). *Int. J. Cancer* **52**, 197-201.

Natali PG, Nicotra MR, Sures I, Mottolese M, Botti C, Ullrich A. (1992b). *Int. J. Cancer*, **52**, 713-717.

Natali PG, Berlingieri MT, Nicotra MR, Fusco A, Santoro E, Bigotti A and Vecchio G. (1995). *Cancer Res.*, **55**, 1787-1791.

Nishida K, Tsukamoto T, Uchida K, Takahashi T, Takahashi T and Ueda R. (1996). *Anticancer Res.*, **16**, 3397-3402.

Okamoto K and Beach D. (1994). *EMBO J.*, **13**, 4816-4622.

Okamoto K and Prives C. (1999). *Oncogene*, **18**, 4606-4615.

Owens GK, Loeb A, Gordon D and Thompson MM. (1986). *J. Cell Biol.*, **102**, 343-352.

Rudland PS, Leinster SJ, Winstanley J, Green B, Atkinson M and Zakhour HD. (1993). *J. Histochem. Cytochem.*, **41**, 543-553.

Polyak K, Xia Y, Zweier JL, Kinzler KW and Vogelstein B. (1997). *Nature*, **389**, 300-305.

Seidenfeld J and Marton LJ. (1979). *J Natl Cancer Inst.*, **63**, 919-931.

Shimizu A, Nishida J, Ueoka Y, Kato K, Hachiya T, Kuriaki Y and Wake N. (1998). *Biochem. Biophys. Res. Commun.*, **242**, 529-533.

Smith ML, Kontny HU, Bortnick R and Fornace AJ Jr. (1997). *Exp. Cell Res.*, **230**, 61-68.

Taylor WR, DePrimo SE, Agarwal A, Agarwal ML, Schonthal AH, Katula KS and Stark GR. (1999). *Mol. Biol. Cell.*, **10**, 3607-3622.

Tsukamoto AS, Grosschedl R, Guzman RC, Parslow T and Varmus HE. (1988). *Cell*, **55**, 619-625.

Wallace-Brodeur RR, Lowe SW. (1999). *Cell Mol Life Sci.*, **55**, 64-75.

Xiong Y, Hannon GJ, Zhang H, Casso D, Kobayashi R and Beach D. (1993). *Nature*, **366**, 701-704.

Yu J, Zhang L, Hwang PM, Rago C, Kinzler KW and Vogelstein B. (1999). *Proc Natl Acad Sci USA*, **96**, 14517-14522.

Zhao R, Gish K, Murphy M, Yin Y, Notterman D, Hoffman WH, Tom E, Mack DH and Levine AJ. (2000). *Genes Dev.*, **14**, 981-993.

Table I. Biological and genetic properties of *Wnt-1* TG p53+/+ and *Wnt-1* TG p53-/- mammary adenocarcinomas

Property	p53+/+	p53-/-
Tumor type	mammary adenocarcinoma	mammary adenocarcinoma
50% tumor incidence	22.5 weeks	11.5 weeks
100% tumor incidence	40 weeks	15 weeks
Mean tumor growth rate	800 cu. mm/wk	3400 cu. mm/wk
Mean percentage of mitotic tumor cells	.0027	.0070
Mean percentage of apoptotic tumor cells	0.32	0.48
Percentage of tumors with abnormal chromosomes	33	100
Mean number of abnormal chromosomes per tumor	0.3	1.7
Histopathological appearance	uniform nuclei differentiated more stroma	anaplastic undifferentiated less stroma

Table II. Differentially expressed genes in *Wnt-1* TG p53+/+ and *Wnt-1* TG p53-/- mammary adenocarcinomas

Gene	ID method	p53+/+ levels	Mean difference	P value	protein	p53 target	Function/Marker
Alpha smooth muscle actin	Diff. Display	Increased	4.25	<0.001	Yes	Yes	myoepithelial marker
Kappa casein	Diff. Display	Increased	3.18	0.045	ND	No	luminal cell epithelial marker
Aldolase C	Diff. Display	Increased	2.87	0.05	ND	No	CNS glycolytic enzyme
c-kit	cDNA Array	Increased	2.38	0.01	Yes	No	receptor tyrosine kinase
Cytokeratin 19	cDNA Array	Increased	2.73	0.003	Yes	Yes	epithelial cell intermediate filament marker
$P21^{WAF1/CIP1}$	Northern	Increased	2.27	0.01	ND	Yes	cdk inhibitor growth marker
Cyclin B1	RNAse Prot	Decreased	2.31	0.04	Yes	Yes	mitotic cyclin growth marker
Cyclin G1	RNAse Prot.	Increased	1.79	0.04	ND	Yes	function unclear poss. growth marker

Figure Legends

Figure 1. Differentially expressed genes in *Wnt-1* TG p53+/+ mice and *Wnt-1* TG p53-/- mice identified by differential display PCR and confirmed by Northern blot hybridizaton. (A) A representative differential display PCR product (T1P5b1, arrow) expressed at higher levels in the *Wnt-1* TG p53+/+ tumors compared to either *Wnt-1* TG p53+/-LOH or *Wnt-1* TG p53-/- tumors. (B) Northern blot results of three genes (alpha smooth muscle actin, kappa casein, and aldolase C) identified by differential display PCR. Eight different tumor RNA samples from each *Wnt-1* TG genotype (p53+/+ and p53-/-) were loaded. After normalizing to the control RNA (GAPDH) signal, significant increases in RNA levels of these three genes are observed in *Wnt-1* TG p53+/+ tumors.

Figure 2. Differentially expressed genes in *Wnt-1* TG p53+/+ and *Wnt-1* TG p53-/- mammary tumors identified by cDNA array analysis. Two genes (c-*kit* and cytokeratin 19) consistently showed differential expression by cDNA array analysis. (A) Representative array showing a strong signal for cytokeratin 19 (CK19) in the *Wnt-1* TG p53+/+ sample compared to the *Wnt-1* TG p53-/- sample. (B) Northern blot hybridization of c-*kit* with 5 RNA samples from *Wnt-1* TG p53+/+ or *Wnt-1* TG p53-/- tumors. The control probe is GAPDH. (C) Northern blot hybridization of cytokeratin 19 (CK19) with 8 tumor samples from each *Wnt-1* TG p53 genotype. After normalization of hybridization signals to control RNA (GAPDH) signals, c-*kit* and CK19 expression are significantly higher on average in *Wnt-1* TG p53+/+ tumors.

Figure 3. Differential expression of the p53-target gene, $p21^{WAF1/CIP1}$, in *Wnt-1* TG p53+/+ and *Wnt-1* TG p53-/- mammary tumors. Northern blot hybridization shows five tumor RNA samples from each p53 genotype loaded for comparison. After normalizing to control (GAPDH) mRNA levels, $p21^{WAF1/CIP1}$ shows significantly higher expression in *Wnt-1* TG p53+/+ tumors than in *Wnt-1* TG p53-/- tumors.

Figure 4. Differentially expressed cyclin RNAs in *Wnt-1* TG p53+/+ and *Wnt-1* TG p53-/- mammary tumors identified by RNAse protection assay. Multi-probe sets specific for murine cyclins A to D (panel A) or cyclins E to H (panel B) were used for the assay. (A) Comparison of six *Wnt-1* TG p53+/+ tumor RNAs and six *Wnt-1* TG p53-/- tumor RNAs by RNAse protection assay for cyclin A2, cyclin B1, cyclin D1, and cyclin D2. After normalization to the GAPDH signal, only cyclin B1 showed significantly higher expression in the p53-/- tumors. (B) Comparison of six *Wnt-1* TG p53+/+ tumor RNAs and five *Wnt-1* TG p53-/- tumor RNAs by RNAse protection assay for cyclins E, F, G1, G2, and H. The cyclin G1 levels in the *Wnt-1* TG p53+/+ tumors are significantly higher on average than in the *Wnt-1* TG p53-/- tumors after normalization to the GAPDH loading control.

Figure 5. Differential expression of proteins in *Wnt-1* TG p53+/+ and *Wnt-1* TG p53-/- mammary tumors as assayed by Western blot analyses. Tumor lysates were subjected to SDS-polyacrylamide gel electrophoresis, followed by transfer to nylon membranes and immunoblotting with antibodies to the various differentially expressed proteins. Each blot was then stripped and immunoblotted with an antibody to vertebrate actin, which served as a loading control. (A) Alpha smooth muscle actin protein expression in six *Wnt-1* TG p53+/+ and six *Wnt-1* TG p53-/- mammary tumor lysates. Alpha smooth muscle actin levels were elevated in *Wnt*-1 TG p53+/+ tumors compared to *Wnt-1* TG p53-/- tumors. (B) c-kit and cytokeratin19 (CK19) proteins in seven *Wnt-1* TG p53+/+ and seven *Wnt-1* TG p53-/- mammary tumor lysates. The *Wnt-1* TG p53+/+ tumors had higher levels of c-kit and CK19 proteins on average compared to their *Wnt-1* TG p53-/- counterparts. (C) Cyclin B1 protein levels in six *Wnt-1* TG p53+/+ and six *Wnt-1* TG p53-/- mammary tumor lysates. *Wnt-1* TG p53-/- tumors exhibited higher mean levels of cyclin B1 than *Wnt-1* TG p53+/+ tumors.

Figure 1

A

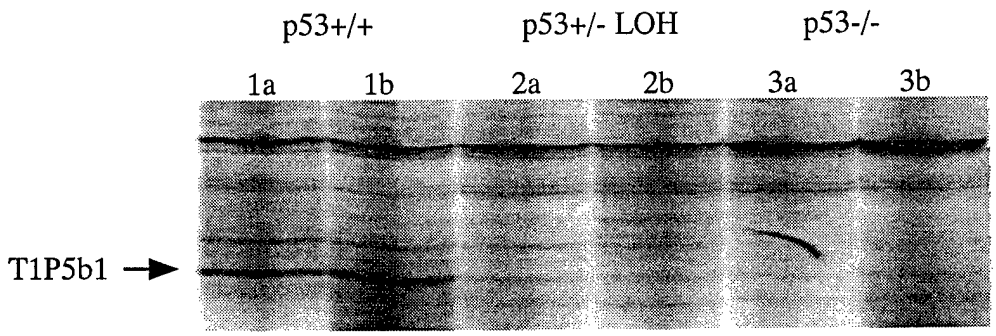
p53+/+
p53+/- LOH
p53-/-
1a
1b
2a
2b
3a
3b
T1P5b1

B

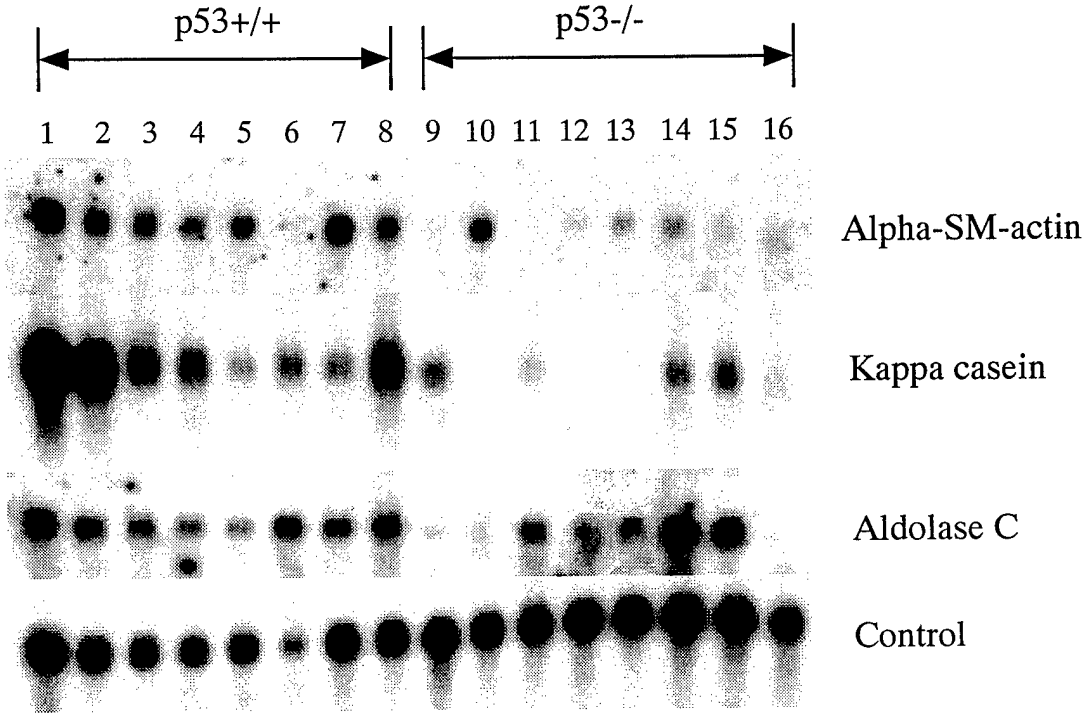
p53+/+
p53-/-
1 2 3 4 5 6 7 8 9 10 11 12 13 14 15 16
Alpha-SM-actin
Kappa casein
Aldolase C
Control

Figure 2

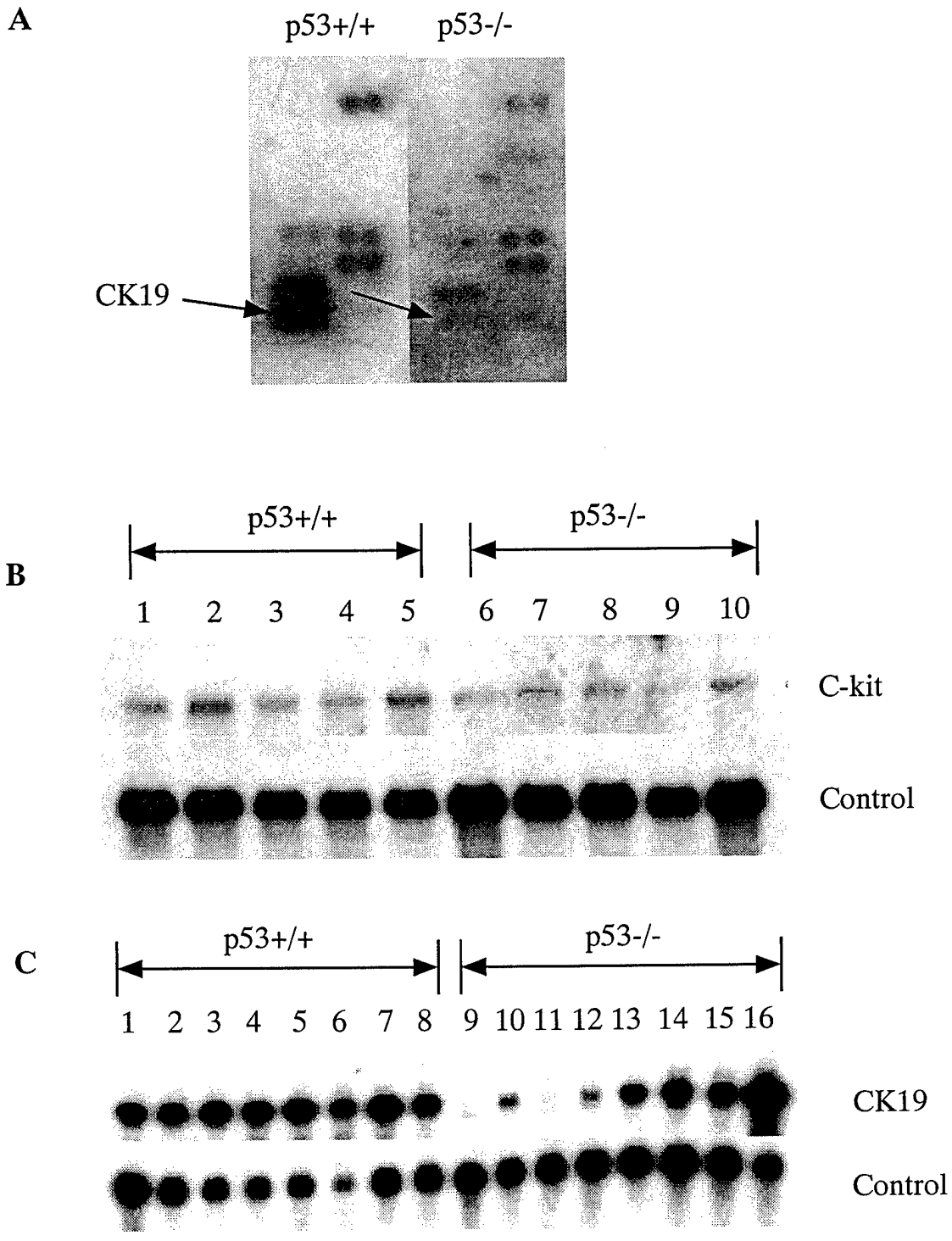
A
p53+/+
p53-/-
CK19
B
p53+/+
p53-/-
1 2 3 4 5 6 7 8 9 10
C-kit
Control
C
p53+/+
p53-/-
1 2 3 4 5 6 7 8 9 10 11 12 13 14 15 16
CK19
Control

Figure 3

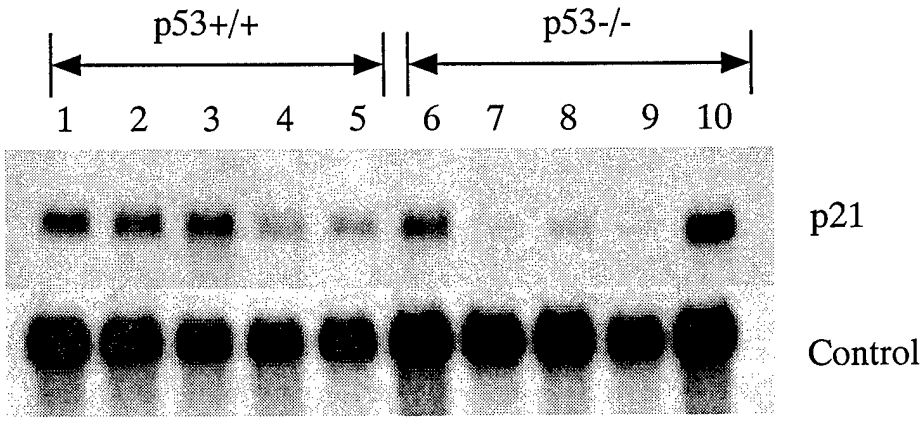

Figure 4

A

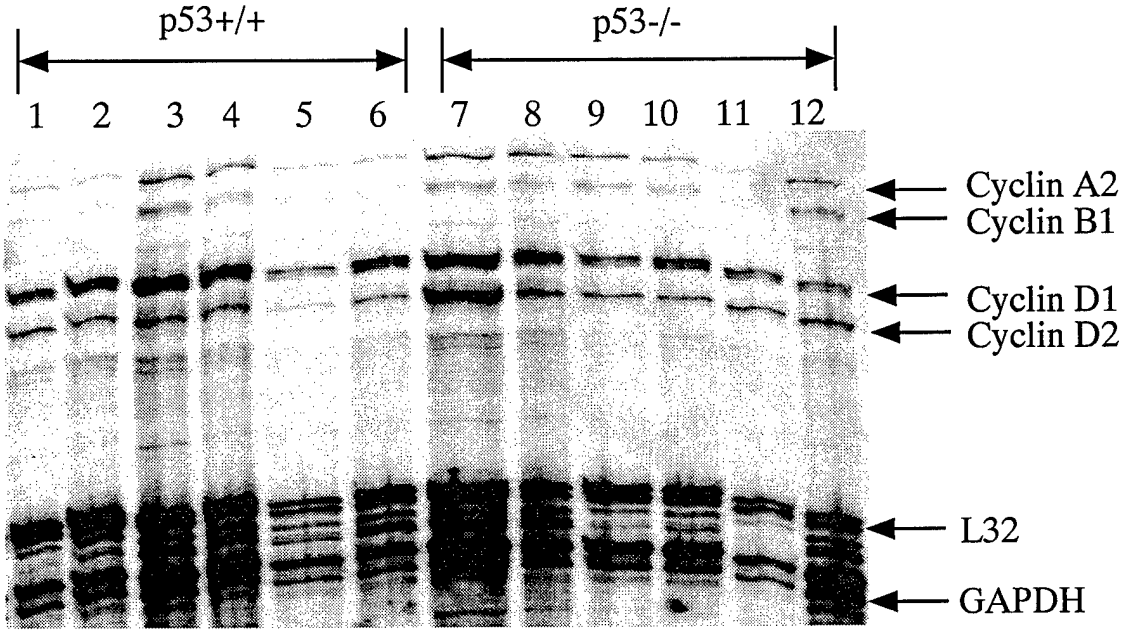
p53+/+
p53-/-
1 2 3 4 5 6 7 8 9 10 11 12
Cyclin A2
Cyclin B1
Cyclin D1
Cyclin D2
L32
GAPDH

B

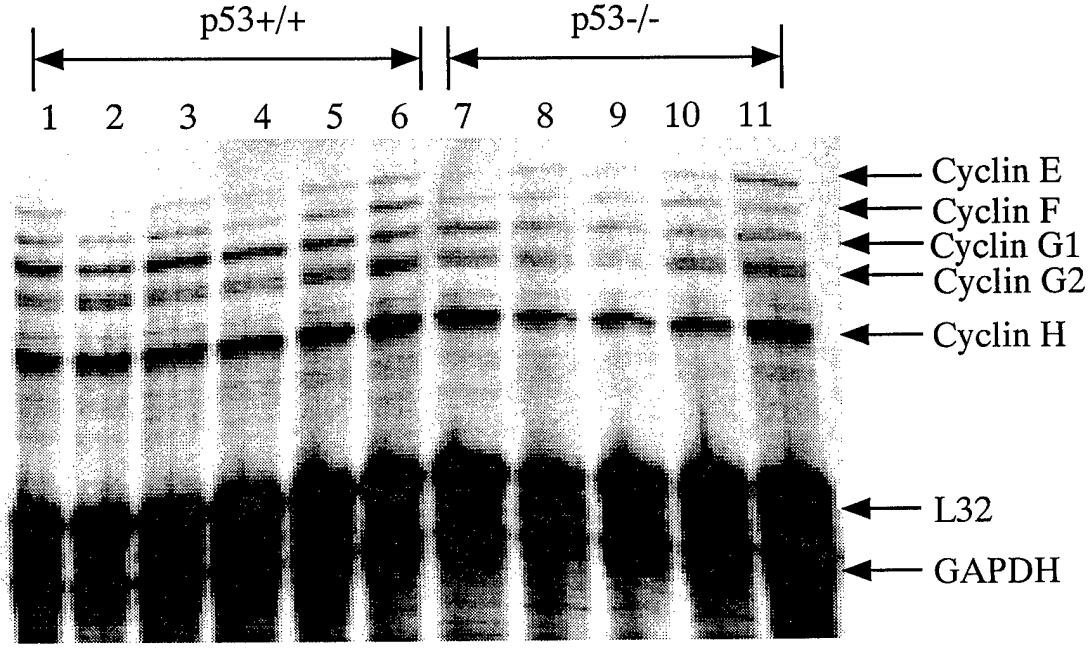
p53+/+
p53-/-
1 2 3 4 5 6 7 8 9 10 11
Cyclin E
Cyclin F
Cyclin G1
Cyclin G2
Cyclin H
L32
GAPDH

Figure 5

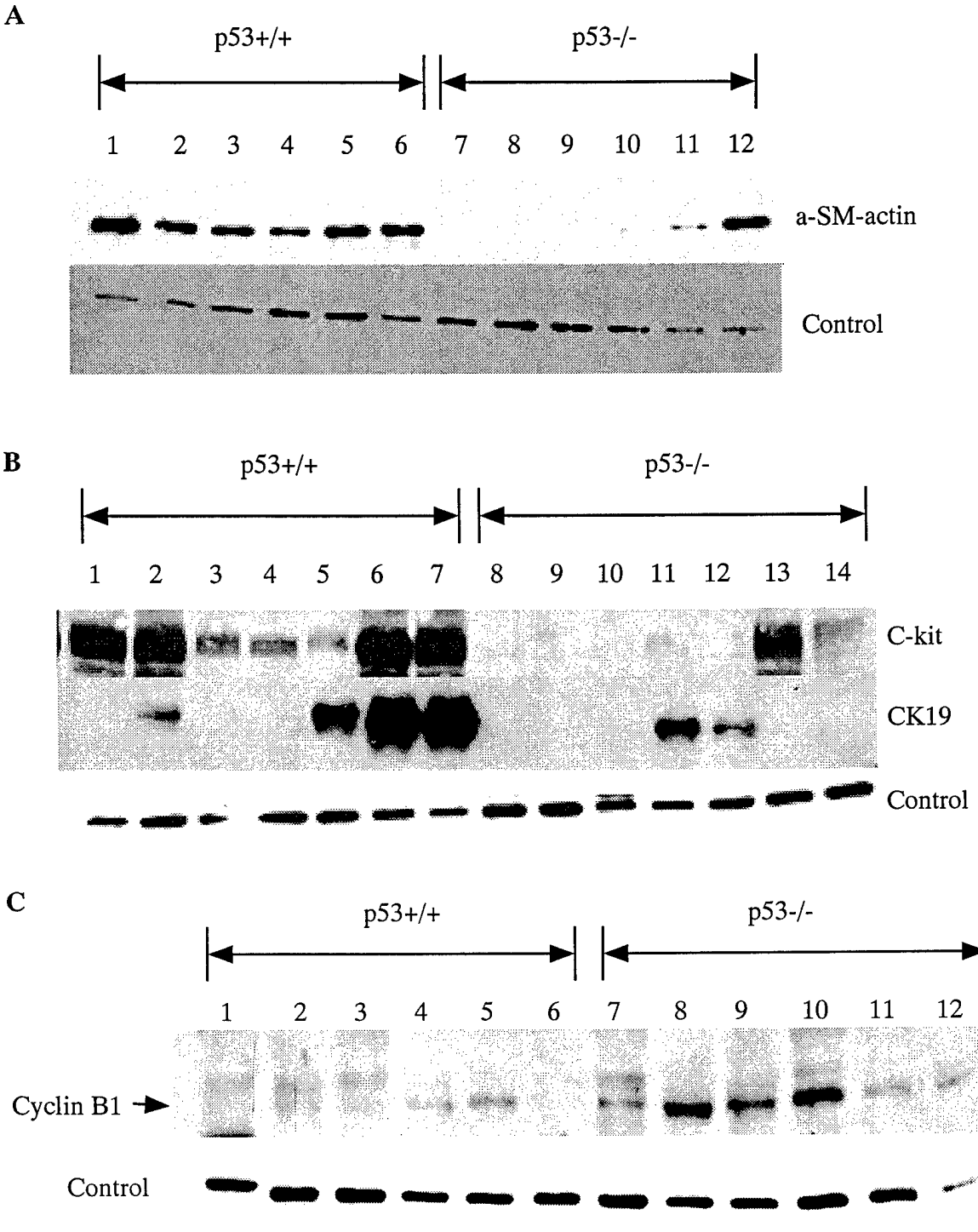
A
p53+/+
p53-/-
1 2 3 4 5 6 7 8 9 10 11 12
a-SM-actin
Control
B
p53+/+
p53-/-
1 2 3 4 5 6 7 8 9 10 11 12 13 14
C-kit
CK19
Control
C
p53+/+
p53-/-
1 2 3 4 5 6 7 8 9 10 11 12
Cyclin B1
Control